

L. Tessé, J.-M. Lamet
(Onera)

E-mail: lionel.tesse@onera.fr

Radiative Transfer Modeling Developed at Onera for Numerical Simulations of Reactive Flows

Radiative flux and power have to be calculated in many applications simulated using CFD, such as the prediction of pollutant emissions and the service life of aero-engine combustors, the design of thermal protection systems and ignition of solid propellant rocket motors, the design of spacecraft heat shields for atmospheric (re-) entries, and so on. In such configurations, the media are composed of gases (combustion products or plasma) and particles (soot, alumina, water droplets). Since the use of a line-by-line approach is not possible in industrial configurations, radiative properties are computed with an approximate band model. For gas radiative properties, this model is formulated either in terms of the absorption coefficient or in terms of transmissivity. To deal with any kind of problems, the Monte Carlo method has been chosen to solve the integral form of the Radiative Transfer Equation (RTE) allowing the use of the two formulations of the gas radiative property model. For media that can be dealt with using a model formulated in terms of the absorption coefficient, the Discrete Ordinates Method (DOM), that solves only the differential form of the RTE, has also been developed since it is reputed to consume less computation time than the Monte Carlo method. In this paper the fundamental relations of thermal radiation are first summarized. Then, both of the numerical methods and all the gas and particle radiative property models used at Onera to solve the RTE are described. Finally, some examples of typical applications studied at Onera with ASTRE (Monte Carlo) and REA (DOM) solvers are presented briefly.

Introduction

In CFD simulations, it is often necessary to compute the radiative fluxes at the calculation domain boundaries and/or the radiative powers in the volume of the domain. Radiative power is equal to the opposite of the radiative flux divergence that appears in the total energy conservation equation of the Navier-Stokes system.

In most flames, radiative transfer significantly influences the temperature field and hence the concentration of reactive species. On the other hand, the radiative power field depends to a great extent on the temperature and the composition of the medium. There is a strong coupling between combustion and radiative transfer, particularly in the presence of soot particles. Therefore it is important to take radiation into account to predict, for instance, the pollutant emissions of an aero-engine combustor. In particular, NO_x formation is very sensitive to the temperature level. Moreover, convective heat fluxes on the combustor walls are considerably reduced with a film cooling technique. This makes radiative heat flux calculation indispensable for a satisfactory prediction of the thermal gradients inside the walls which govern combustor service life.

A second kind of application in which radiation plays a significant role is aluminized solid propellant rocket engines. In order to protect the structural parts of the motor several types of thermal protecting materials are used. The prediction of convective and radiative fluxes on these materials is important since the flux levels directly affect performance (ablation in the nozzle throat, impulse to weight ratio) and the safety of the motor. The flux levels may be of the order of several MWm⁻² and radiative contributions, from combustion gases and alumina particles, range from practically 100% (internal parts) to about 10% (divergent part of the nozzle). Moreover, it has been shown that radiative fluxes have a strong effect on the ignition of a solid rocket motor, due to the radiative heat feedback on the propellant surface, which is a significant fraction of the total heat feedback.

A last example of possible applications is atmospheric (re-)entries. High velocities encountered in these kinds of flows (up to 12 km/s for Earth re-entry) lead to the formation of a shock in front of the heat shield of the spacecraft. Gases behind the shock can be ionized, dissociated and under chemical and thermal nonequilibrium conditions. High rotational, vibrational and electronic temperatures give rise to a strong radiative emission in the shock layer, which increases

the heat flux on the surface of the spacecraft. Kinetics and radiative transfer are strongly coupled because both depend on energy state populations. Therefore, the radiative transfer needs to be computed to be able to predict the shock layer position and design the heat shield. Moreover, in the Mars Premier project, preliminary computations tended to prove that the effects of radiation heating could be crucial during the aerocapture phase in the Martian atmosphere. As a matter of fact, radiation emitted in the wake region of the orbiter could overheat the payload and put a question mark over the technology of the thermal protection system.

For a given configuration, the most suitable gas radiative property model depends on the thermophysical conditions. If a gas radiative property model formulated in terms of transmissivity is needed, it is the integral form of the RTE (Radiative Transfer Equation) that has to be solved. If a model formulated in terms of the absorption coefficient can be used then the integral and the differential forms of the RTE can be solved since transmissivities can be obtained from the absorption coefficients. Therefore, two numerical methods have been developed at Onera: the Discrete Ordinates Method (DOM) and the Monte Carlo method. The first offers a good compromise between accuracy and CPU time, but it solves only the differential form of the RTE with a gas radiative property model formulated in terms of the absorption coefficient. Moreover, its use requires some assumptions about physical phenomena modeling (impossible to take into account spectral correlations and turbulence-radiation interaction for example). The Monte Carlo method is a powerful tool that can be used to solve any kind of problem since it solves the integral form of the RTE, but this statistical method has a reputation for its heavy consumption of CPU time.

The paper is divided into five parts. The first part goes over the fundamental relations of thermal radiation and the second describes two numerical methods used at Onera to solve the RTE. The third and fourth parts focus on gas and particle radiative property models. The last part then briefly presents the available models and typical applications studied at Onera with ASTRE (Monte Carlo) and REA (DOM) solvers.

Fundamental relations of thermal radiation

Consider a participating medium enclosed by opaque walls and characterized by a refractive index equal to unity (this assumption is valid in most of the gas flows studied at Onera). At any point M of this three-dimensional system (volume and boundaries), the radiative flux vector can be defined as:

$$\vec{q}^R(M) = \int_0^{+\infty} \int_{4\pi} I_\nu(M, \vec{u}) \vec{u} d\Omega d\nu \quad (1)$$

where ν is the wavenumber (m^{-1}), \vec{u} a unit direction vector, $d\Omega$ an infinitesimal solid angle (Sr) around the direction \vec{u} and $I_\nu(M, \vec{u})$ the directional monochromatic radiative intensity ($Wm^{-2}Sr^{-1}(m^{-1})^{-1}$). This intensity represents the radiative energy flow per unit time, unit solid angle, unit wavenumber and unit area normal to the considered direction.

From the definition of the radiative flux vector, expressions of wall radiative flux ϕ^R (Wm^{-2}) and of radiative power P^R (Wm^{-3}) can be derived:

$$\phi^R(B) = -\vec{q}^R(B) \cdot \vec{n}_B = - \int_0^{+\infty} \int_{4\pi} I_\nu(B, \vec{u}) \vec{u} \cdot \vec{n}_B d\Omega d\nu \quad (2)$$

$$P^R(M) = -[\vec{\nabla} \cdot \vec{q}^R]_M = - \int_0^{+\infty} \int_{4\pi} \left[\frac{\partial I_\nu(s, \vec{u})}{\partial s} \right]_{s=s_M} d\Omega d\nu \quad (3)$$

where B is a point on boundaries, \vec{n}_B the unit surface normal at the point B (pointing away from the surface into the medium) and M a point in the medium. The radiative power is equal to the opposite of the radiative flux divergence that appears in the total energy conservation equation of the Navier-Stokes system. The wall radiative flux is needed to solve heat conduction problems inside the walls.

The integral over the solid angle in equation (2) can be split into two parts: directions pointing towards the surface (incident radiation impinging onto the surface and absorbed by the wall) and directions pointing outwards from the surface into the medium (radiation emitted by the wall). This gives:

$$\phi^R(B) = \underbrace{\int_0^{+\infty} \int_{2\pi(\vec{u} \cdot \vec{n}_B < 0)} \alpha_\nu(B, \vec{u}) I_\nu^{inci}(B, \vec{u}) |\vec{u} \cdot \vec{n}_B| d\Omega d\nu}_{\text{absorption}} - \underbrace{\int_0^{+\infty} \int_{2\pi(\vec{u} \cdot \vec{n}_B > 0)} I_\nu^{emi}(B, \vec{u}) |\vec{u} \cdot \vec{n}_B| d\Omega d\nu}_{\text{emission}} \quad (4)$$

where $I_\nu^{inci}(B, \vec{u})$ and $I_\nu^{emi}(B, \vec{u})$ are, respectively, the incident directional monochromatic radiative intensity ($Wm^{-2}Sr^{-1}(m^{-1})^{-1}$) impinging onto the surface at the point B and the directional monochromatic intensity emitted by the wall at the point B . Under the assumption of Local Thermodynamic Equilibrium (LTE means that relaxation processes occur rapidly in such a way that the energy states are populated according to Boltzmann's distribution) $I_\nu^{emi}(B, \vec{u})$ can be expressed as the product $\epsilon_\nu(B, \vec{u}) I_\nu^o(T_B)$ and the directional monochromatic absorptivity $\alpha_\nu(B, \vec{u})$ is taken to be equal to the directional monochromatic emissivity $\epsilon_\nu(B, \vec{u})$. $I_\nu^o(T_B)$ is the monochromatic equilibrium (or blackbody) intensity ($Wm^{-2}Sr^{-1}(m^{-1})^{-1}$) and T_B is the wall temperature at point B (K). $I_\nu^o(T)$ is also called the Planck function and is written:

$$I_\nu^o(T) = \frac{2hc_0^2 \nu^3}{e^{hc_0\nu/kT} - 1} \quad (5)$$

where $h = 6.6261 \times 10^{-34}$ Js is Planck's constant, $c_0 = 2.998 \times 10^8$ ms⁻¹ is the speed of light in the vacuum and $k = 1.3807 \times 10^{-23}$ JK⁻¹ is Boltzmann's constant. Emission by solid walls is characterized by equilibrium intensity because, in all the CFD simulations performed at Onera, solids can be considered to be at LTE.

Equations (3) and (4) show that it is necessary to know the field of directional monochromatic intensity $I_\nu(s, \vec{u})$ to be able to compute radiative power and flux. This field can be obtained by solving the Radiative Transfer Equation (RTE) which describes the change of the radiative intensity along a ray. The differential form of the RTE is obtained by making an energy balance on the radiative energy traveling in the direction \vec{u} between the locations s and $s + ds$. This leads to:

$$\frac{\partial I_\nu(s, \bar{u})}{\partial s} = \underbrace{\eta_\nu(s) + \frac{\sigma_\nu(s)}{4\pi} \int_{4\pi} I_\nu(s, \bar{u}') \Phi_\nu(s, \bar{u}' \rightarrow \bar{u}) d\Omega'}_{\text{gain by emission and incoming scattering}} - \underbrace{(\kappa_\nu(s) + \sigma_\nu(s)) I_\nu(s, \bar{u})}_{\text{loss by absorption and scattering}} \quad (6)$$

where η_ν is the monochromatic emission coefficient ($\text{Wm}^{-2}\text{Sr}^{-1}$), κ_ν the monochromatic absorption coefficient (m^{-1}) and σ_ν the monochromatic scattering coefficient (m^{-1}). These three coefficients are considered to be isotropic. The quantity $\Phi_\nu(s, \bar{u}' \rightarrow \bar{u})$ is called the scattering phase function and describes the angular distribution of the scattered intensity. $\Phi_\nu(s, \bar{u}' \rightarrow \bar{u}) d\Omega' / 4\pi$ can be interpreted as the probability of a ray, propagating in direction \bar{u}' , to be scattered in the direction \bar{u} at location s .

The transient form of the RTE is not presented here. The transient term on the left-hand side of equation (6) has been neglected because, for the vast majority of flows studied at Onera, the characteristic time of radiation propagation is very small compared to the characteristic times of the other physical phenomena involved.

Equation (6) can be rewritten in order to be integrated over an optical thickness from a point $s' = s_{B_0}$ at the wall to a point $s' = s$ inside the medium, giving:

$$I_\nu(s, \bar{u}) = \underbrace{I_\nu^{leav}(s_{B_0}, \bar{u}) \tau_\nu(s_{B_0}, s)}_{\text{part due to wall}} + \underbrace{\int_{s_{B_0}}^s S_\nu(s', \bar{u}) \tau_\nu(s', s) ds'}_{\text{part due to source function along the optical path}} \quad (7)$$

where $S_\nu(s', \bar{u})$ is the source function (emission and incoming scattering) defined as:

$$S_\nu(s', \bar{u}) = \eta_\nu(s') + \frac{\sigma_\nu(s')}{4\pi} \int_{4\pi} I_\nu(s', \bar{u}') \Phi_\nu(s', \bar{u}' \rightarrow \bar{u}) d\Omega' \quad (8)$$

and $\tau_\nu(s', s)$ is the monochromatic transmissivity given by:

$$\tau_\nu(s', s) = \exp\left[-\int_{s'}^s (\kappa_\nu(s'') + \sigma_\nu(s'')) ds''\right] \quad (9)$$

Equation (7) is known as the integral form of the RTE. This equation is interpreted physically as the monochromatic intensity, at location s in direction \bar{u} , being composed of two terms. The first is the contribution of intensity leaving the wall (or entering the enclosure if it is an open boundary), which decays exponentially due to extinction (absorption and scattering) over the optical distance $\|s - s_{B_0}\|$. The second term results from emission and incoming scattering in the direction \bar{u} by all the elements ds' along the path from s_{B_0} to s , reduced by exponential attenuation between each location of emission and incoming scattering s' and the location s .

The monochromatic intensity leaving the wall at point B_0 in direction \bar{u} can be expressed as the sum of emitted and reflected intensities, given by:

$$I_\nu^{leav}(B_0, \bar{u}) = \varepsilon_\nu(B_0, \bar{u}) I_\nu^o(T_{B_0}) + (1 - \varepsilon_\nu(B_0, \bar{u})) I_\nu^{inci}(B_0, \bar{u}^*) \quad (10)$$

if the wall is a specularly reflecting surface; $-\bar{u}^*$ is the symmetrical direction of \bar{u} about \bar{n}_{B_0} . If the wall is a diffusively reflecting surface, equation (10) becomes:

$$I_\nu^{leav}(B_0, \bar{u}) = \varepsilon_\nu(B_0) I_\nu^o(T_{B_0}) + \frac{1 - \varepsilon_\nu(B_0)}{\pi} \int_{2\pi(\bar{u} \cdot \bar{n}_{B_0} < 0)} I_\nu^{inci}(B_0, \bar{u}') |\bar{u}' \cdot \bar{n}_{B_0}| d\Omega' \quad (11)$$

Finally, the expressions for the radiative flux and power are obtained respectively by substituting equation (7) into equation (4) and equation (6) into equation (3). This leads to:

$$\varphi^R(B) = \underbrace{\int_0^{+\infty} \int_{2\pi(\bar{u} \cdot \bar{n}_B < 0)} \alpha_\nu(B, \bar{u}) \left[I_\nu^{leav}(B_0, \bar{u}) \tau_\nu(s_{B_0}, s_B) + \int_{s_{B_0}}^{s_B} S_\nu(s', \bar{u}) \tau_\nu(s', s_B) ds' \right] |\bar{u} \cdot \bar{n}_B| d\Omega d\nu}_{\text{absorption}} - \underbrace{\int_0^{+\infty} I_\nu^o(T_B) \int_{2\pi(\bar{u} \cdot \bar{n}_B > 0)} \varepsilon_\nu(B, \bar{u}) |\bar{u} \cdot \bar{n}_B| d\Omega d\nu}_{\text{emission}} \quad (12)$$

$$P^R(M) = \underbrace{\int_0^{+\infty} \kappa_\nu(M) \int_{4\pi} I_\nu(M, \bar{u}) d\Omega d\nu}_{\text{absorption}} - \underbrace{4\pi \int_0^{+\infty} \eta_\nu(M) d\nu}_{\text{emission}} \quad (13)$$

When the medium is a mixture of gases and particles, the monochromatic absorption coefficient of the medium is given by:

$$\kappa_\nu(M) = \kappa_\nu^{gas}(M) + \kappa_\nu^{part}(M) \quad (14)$$

The monochromatic scattering coefficient and the monochromatic scattering phase function are only due to particles in the medium. Scattering by gas molecules is never taken into account in CFD simulations since its effect on heat radiative transfer is always negligible in the considered applications.

Combination of equations (9) and (14) leads to:

$$\tau_\nu(s', s) = \exp\left[-\int_{s'}^s \kappa_\nu^{gas}(s'') ds''\right] \times \exp\left[-\int_{s'}^s (\kappa_\nu^{part}(s'') + \sigma_\nu(s'')) ds''\right] = \tau_\nu^{gas}(s', s) \times \tau_\nu^{part}(s', s) \quad (15)$$

When a gas radiative property model formulated in terms of transmissivity is used, equation (13) cannot be used directly. Another expression for the radiative power can be obtained by substituting equation (7) into equation (13), giving:

$$P^R(M) = \underbrace{\int_0^{+\infty} \kappa_\nu(M) \int_{4\pi} \left[I_\nu^{leav}(B_0, \bar{u}) \tau_\nu(s_{B_0}, s_M) + \int_{s_{B_0}}^{s_M} S_\nu(s', \bar{u}) \tau_\nu(s', s_M) ds' \right] d\Omega d\nu}_{\text{absorption}} - \underbrace{4\pi \int_0^{+\infty} \eta_\nu(M) d\nu}_{\text{emission}} \quad (16)$$

It is worth noticing that the multiplication of equation (14) by equation (15) results in:

$$\begin{aligned} \kappa_\nu(s)\tau_\nu(s',s) &= \kappa_\nu^{gas}(s)\tau_\nu^{gas}(s',s)\tau_\nu^{part}(s',s) + \kappa_\nu^{part}(s)\tau_\nu(s',s) \\ &= -\frac{\partial \tau_\nu^{gas}(s',s)}{\partial s}\tau_\nu^{part}(s',s) + \kappa_\nu^{part}(s)\tau_\nu(s',s) \end{aligned} \quad (17)$$

Using relation (17) in equation (16) we obtain:

$$\begin{aligned} P^R(M) &= \int_0^{+\infty} \int_{4\pi} \left[\begin{array}{l} -\frac{\partial \tau_\nu^{gas}(s_{B_0},s)}{\partial s} \Big|_{s=s_M} \tau_\nu^{part}(s_{B_0},s_M) \\ + \kappa_\nu^{part}(s_M)\tau_\nu(s_{B_0},s_M) \end{array} \right] I_\nu^{leav}(B_0,\bar{u}) \\ &\quad + \int_{s_{B_0}}^{s_M} \left[\begin{array}{l} -\frac{\partial \tau_\nu^{gas}(s',s)}{\partial s} \Big|_{s=s_M} \tau_\nu^{part}(s',s_M) \\ + \kappa_\nu^{part}(s_M)\tau_\nu(s',s_M) \end{array} \right] S_\nu(s',\bar{u}) ds' \\ &\quad \underbrace{\hspace{10em}}_{\text{absorption}} \Big] d\Omega d\nu \\ &= \underbrace{-4\pi \int_0^{+\infty} \eta_\nu(M) d\nu}_{\text{emission}} \end{aligned} \quad (18)$$

Equation (18) is useful when a gas radiative property model formulated in terms of transmissivity is used because the gas absorption coefficient does not appear.

Assuming LTE (it is usually the case for combustion applications but not always for atmospheric entry flows), the monochromatic emission coefficient of the medium can be written:

$$\eta_\nu(M) = \kappa_\nu^{gas}(M)I_\nu^o(T_M^{gas}) + \sum_{k=1}^{N_{part}} \kappa_\nu^{p,k}(M)I_\nu^o(T_M^{p,k}) \quad (19)$$

where N_{part} is the number of particle sizes considered in the simulation. These particles can be in thermal nonequilibrium with the gases.

When the medium does not contain particles or particles are not taken into account in radiative transfer calculation, relation (18) can be expressed more simply as:

$$\begin{aligned} P^R(M) &= \int_0^{+\infty} \int_{4\pi} \left[\begin{array}{l} -\frac{\partial \tau_\nu^{gas}(s_{B_0},s)}{\partial s} \Big|_{s=s_M} I_\nu^{leav}(B_0,\bar{u}) \\ + \int_{s_{B_0}}^{s_M} \frac{\eta_\nu(s')}{\kappa_\nu(s')} \frac{\partial^2 \tau_\nu^{gas}(s',s)}{\partial s \partial s'} \Big|_{s=s_M} ds' \end{array} \right] d\Omega d\nu \\ &\quad \underbrace{\hspace{10em}}_{\text{absorption}} \\ &= \underbrace{-4\pi \int_0^{+\infty} \eta_\nu(M) d\nu}_{\text{emission}} \end{aligned} \quad (20)$$

where the ratio η_ν / κ_ν can be replaced by the Planck function, given by equation (5), at LTE conditions.

All the previous equations involve monochromatic quantities, but in practical cases such as industrial configurations, it is not possible to perform line by line calculations since this approach requires more than 10^6 spectral points. Therefore it is necessary to average these equations over a spectral interval and to use a radiative property model providing quantities averaged over a spectral band. However, it is not always easy to write the averaged equations in a form that is suitable for the quantities given by the radiative property model. Sometimes it is not possible to take into account spectral correlations between radiative quantities.

When radiative transfer occurs in turbulent flows then turbulence-radiation interaction (TRI) has to be taken into account (see Box 1).

Numerical methods developed at Onera

Several numerical methods can be used to compute radiative transfer [23], [32]. Two of them have been developed at Onera: the Monte Carlo method in the ASTRE solver and the discrete ordinates method in the REA solver. These two solvers are included in the CEDRE code [6].

The following two sections describe the two numerical methods. The reader should bear in mind that, to facilitate comprehension, the expressions in this part involve monochromatic radiative properties. However, in the ASTRE and REA solvers, these methods have been used in association with spectral band models, which are explained in the following parts.

Monte Carlo method

Monte Carlo is a generic name for a large class of statistical numerical methods based on a sampling technique. Applied to thermal radiation problems, this kind of method consists in following a finite large number of "energy bundles" through their transport histories, from their points of emission to their points of absorption. An energy bundle is a discrete amount of power (W), which can be thought of as a group of photons bound together. Bundle characteristics (wavenumber, initial direction, point of emission) and physical events along bundle trajectories (absorption, scattering, reflection off walls) are chosen according to probability distributions by drawing random numbers. This is why Monte Carlo simulations are often referred as direct simulations of radiative transfer by statistical distributions of energy over space, direction and wavelength, and results obtained with Monte Carlo methods are often considered as reference solutions. As Monte Carlo methods are statistical, exact results can be approached if enough bundles are followed. Another advantage of Monte Carlo methods is that even the most complicated problem can be solved with relative ease.

As the Monte Carlo method applied to thermal radiation problems consists in emitting, following and absorbing energy bundles (in a similar way to what happens to a photon), the equations solved are not exactly those presented in the previous part. In particular, the source function along the bundle trajectories is taken to be equal to zero: only absorption and direction changes by scattering are considered.

Box 1 - Turbulence-Radiation Interaction (TRI)

In the first section of this article, the transient term of the Radiative Transfer Equation (RTE, see equation (6)) has been neglected because, for the vast majority of flows, the characteristic time of radiation propagation is very small compared to the characteristic times of the other physical phenomena involved. This means that radiation is instantaneous compared to the other physical phenomena, like turbulence, combustion, convection or conduction. Therefore it appears that a model of the Turbulence-Radiation Interaction (TRI) is needed when a radiative transfer calculation is coupled with a turbulent combustion computation, based on a Reynolds-Averaged Navier-Stokes (RANS) approach, which provides only time-averaged quantities. In Large Eddy Simulation (LES), taking into account TRI, is a less crucial problem because only the effects of the subgrid scale fluctuations on radiation have to be modeled.

To simplify the equations, let us take a turbulent flow which can be considered as a non scattering medium at Local Thermodynamic Equilibrium (LTE), like a turbulent sooty flame. Under these assumptions and without taking into account TRI, the RTE is written:

$$\frac{\partial I_\nu(s, \bar{u})}{\partial s} = \kappa_\nu (\langle T(s) \rangle, \langle P(s) \rangle, \langle f_\nu(s) \rangle, \langle x_i(s) \rangle) [I_\nu^o (\langle T(s) \rangle) - I_\nu(s, \bar{u})] \quad (I-1)$$

where $\langle T(s) \rangle$, $\langle P(s) \rangle$, $\langle f_\nu(s) \rangle$ and $\langle x_i(s) \rangle$ are, respectively, the time-averaged temperature, pressure, soot volume fraction and molar fractions of species contributing to radiation. The calculations for the radiative properties and intensities are based on time-averaged quantities. When TRI is taken into account, the RTE that has to be considered becomes:

$$\frac{\partial \langle I_\nu(s, \bar{u}) \rangle}{\partial s} = \langle \kappa_\nu(s) I_\nu^o(s) \rangle - \langle \kappa_\nu(s) I_\nu(s, \bar{u}) \rangle \quad (I-2)$$

This equation shows that two correlations are required: the correlations between absorption coefficient fluctuations and those of equilibrium intensity (given by equation (5) and very sensitive to temperature fluctuations) and between absorption coefficient fluctuations and those of incident radiative intensity. If the fluctuations of T, P, f_ν and x_i are known then it is not difficult to model the first correlation because it involves two terms which depend only on local quantity fluctuations (single-point statistics). Modeling the second correlation is more complex because the incident radiative intensity, given by equation (7), depends on quantity fluctuations in all the cells crossed by the optical path. That is why TRI is very often partially taken into account by assuming:

$$\langle \kappa_\nu(s) I_\nu(s, \bar{u}) \rangle \approx \langle \kappa_\nu(s) \rangle \langle I_\nu(s, \bar{u}) \rangle \quad (I-3)$$

This assumption, commonly called the Optically Thin Fluctuation Approximation (OTFA) in the literature, is valid when, for all wavenumbers ν :

$$\langle \kappa_\nu(s) \rangle \Lambda \ll 1, \quad (I-4)$$

where Λ is the characteristic dimension of large turbulent eddies (or turbulence length scale). Due to the significant dynamics of gas spectra (see for example Figure 1 or 4) it is difficult to evaluate the error generated by the use of the OTFA.

It is worth noticing that some authors [21][22][37] have developed methodologies to take into account full TRI; i.e., with the two fluctuation correlation terms in equation (I-2). For more information about studies dealing with TRI, the reader should consult this review article [4].

TRI is still a current topic of research. Recent studies [8] [30] use Direct Numerical Simulations (DNS) in order to model the effects of the subgrid scale fluctuations on radiation in LES.

To emphasize the principle of the Monte Carlo method, assumptions that simplify the equations are considered in the paragraphs that follow. First, a gas radiative property model formulated in terms of the absorption coefficient is used. To see an example of the implementation in a Monte Carlo method of a gas radiative property model formulated in terms of transmissivity, the reader may refer to the work of Rouzaud et al. [31] or the thesis of Lamet [17]. Secondly, turbulence-radiation interaction (TRI) is not taken into account here, but the thesis of Tessé [35] [37] deals with this subject. Finally, only the conventional Forward Method (FM) is presented here. For informa-

tion about reverse, backward or reciprocal methods the reader should consult references [12], [23], [36] respectively.

Moreover, in order to reduce the variance, the pathlength method [12], also called "energy partitioning" [23], is used. The random number generation, to determine the pathlength traveled before total absorption of an energy bundle, is replaced by the calculation of exponential absorption along the path. Therefore, a bundle contributes to every cell it traverses. A bundle is traced until it either leaves the enclosure or until its energy is depleted below a given cutoff level.

Consider an enclosure filled by a nonisothermal, heterogeneous, absorbing, emitting and scattering media and discretized into N_V volume and N_S surface elements. Each element is supposed to be isothermal and homogeneous and radiative properties, except the phase function, are assumed to be isotropic.

The Monte Carlo statistical estimation of the radiative power in an arbitrary volume element q is written:

$$\tilde{P}_q^{FM} = \frac{1}{V_q} \left[\sum_{i=1}^{N_V+N_S} \tilde{P}_{iq}^{ea} - P_q^e \right] \quad (21)$$

where V_q is the volume of element q and \tilde{P}_{iq}^{ea} the statistical estimation of the power emitted by the element i and absorbed by the volume element q . P_q^e is the power emitted by the volume q defined by:

$$P_q^e = \int_{V_q} \int_{4\pi} \int_0^{+\infty} \eta_{qv} dv d\Omega dV = 4\pi V_q \int_0^{+\infty} \eta_{qv} dv \quad (22)$$

since an element is considered to be isothermal and homogeneous and the spectral emission coefficient η_v is assumed to be isotropic.

The statistical estimation of the power emitted by the cell i and absorbed by the volume element q is written:

$$\tilde{P}_{iq}^{ea} = \frac{P_i^e}{N_i} \sum_{n=1}^{N_{iq}} \sum_{c=1}^{N_{pqn}} \tau_{v_n}(E_{in}, F_{qcn}) \alpha_{qcv_n} \quad (23)$$

where P_i^e is the power emitted by the element i , N_i the total number of bundles leaving the cell i and P_i^e/N_i the initial power of a bundle leaving the cell i . N_{iq} represents the number of bundles leaving the cell i and reaching the volume element q and N_{pqn} the total number of crossings of the volume q by the n^{th} bundle path issued from the element i . $\tau_{v_n}(E_{in}, F_{qcn})$ is the spectral transmissivity between the emission point E_{in} and F_{qcn} the c^{th} inlet point in the volume q of the n^{th} bundle path. The spectral transmissivity is given by:

$$\tau_{v_n}(E_{in}, F_{qcn}) = \exp\left(-\sum_{m=1}^{M_{qcn}-1} \kappa_{mv_n} \ell_m\right) \prod_{h=1}^{N_{rc}} (1 - \varepsilon_{hv_n}) \quad (24)$$

where ℓ_m is the distance traveled through the volume element m and κ_{mv_n} the spectral absorption coefficient in the volume element m . $m=1$ and $m=M_{qcn}$ correspond respectively to the first volume element crossed by the bundle path and the last one for the c^{th} crossing (the volume element q). N_{rc} is the number of wall reflections along the bundle path between the points E_{in} and F_{qcn} , h the index of wall reflections along this bundle path and ε_{hv_n} the local wall spectral emissivity.

The spectral absorptivity α_{qcv_n} is given by:

$$\alpha_{qcv_n} = 1 - \exp(-\kappa_{qv_n} \ell_{qc}) \quad (25)$$

where ℓ_{qc} represents the length of the c^{th} crossing of the volume element q by the bundle path.

If the cell q is a surface element, the volume V_q is replaced by the area A_q in equation (22) and the spectral absorptivity α_{qcv_n} is replaced by the diffuse spectral emissivity ε_{qv_n} in equation (23). Moreover, the power emitted by the cell q becomes:

$$P_q^e = \pi A_q \int_0^{+\infty} \varepsilon_{qv_n} I_v^o(T_q) dv \quad (26)$$

The number of bundles leaving the cell i is determined according to either:

$$N_i = \frac{N}{N_V + N_S} \quad (27)$$

or:

$$N_i = \frac{P_i^e}{\sum_{k=1}^{N_V+N_S} P_k^e} N \quad (28)$$

where N is the total number of bundles involved in the simulation. Equation (27) ensures a spatial uniform distribution of the bundles, while the initial power of a bundle is almost the same for all the bundles with equation (28).

Bundle characteristics (the emission point E inside cell, the polar and azimuthal angles θ and φ characterizing the initial direction and the wavenumber ν) and scattering events along bundle trajectories are considered to be random variables. Therefore, they are chosen according to probability distributions by drawing random numbers in the range 0 to 1 and by assuming these random numbers to be equal to a suitable cumulative distribution functions, i.e.:

$$R_{X_n} = \int_{X_{\min}}^{X_n} f(X) dX \quad (29)$$

where X_n represents the randomly chosen value of the random variable X , R_{X_n} a random number uniformly drawn in the interval [0;1] and $f(X)$ the Probability Density Function (PDF) of the random variable X .

For a volume element i , the joint PDF $f_i(E, \theta, \varphi, \nu)$, based on emission, is obtained from the following relations:

$$f_i(E, \theta, \varphi, \nu) dV_i d\theta d\varphi d\nu = \frac{\eta_{iv} dV_i d\Omega d\nu}{\int_{V_i} \int_{4\pi} \int_0^{+\infty} \eta_{iv} dv d\Omega dV} = \frac{1}{\int_{V_i} dV} dV_i \frac{\sin\theta}{\int_0^\pi \sin\theta' d\theta'} d\theta \frac{1}{\int_0^{2\pi} d\varphi'} d\varphi \frac{\eta_{iv}}{\int_0^{+\infty} \eta_{iv} dv'} dv \quad (30)$$

$$f_i(E, \theta, \varphi, \nu) dV_i d\theta d\varphi d\nu = \frac{1}{V_i} dV_i \frac{\sin\theta}{2} d\theta \frac{1}{2\pi} d\varphi \frac{\eta_{iv}}{\int_0^{+\infty} \eta_{iv} dv'} dv \quad (31)$$

where $d\Omega = \sin\theta d\theta d\varphi$ is an infinitesimal solid angle. Equation (31) shows that the joint PDF $f_i(E, \theta, \varphi, \nu)$ can be factored into a product of the four marginal PDF, i.e.:

$$f_i(E, \theta, \varphi, \nu) dV_i d\theta d\varphi d\nu = f_{i1}(E) dV_i \times f_{i2}(\theta) d\theta \times f_{i3}(\varphi) d\varphi \times f_{i4}(\nu) dv \quad (32)$$

since the emission point E , the two angles θ and φ and the wavenumber ν are statistically independent due to some assumptions (an element is considered as isothermal and homogeneous and the spectral emission coefficient η_v is assumed to be isotropic).

For a diffuse surface element i , equation (31) becomes:

$$f_i(E, \theta, \varphi, \nu) dA_i d\theta d\varphi d\nu = \frac{1}{A_i} dA_i 2 \cos \theta \sin \theta d\theta \frac{1}{2\pi} d\varphi \frac{\varepsilon_{iv} I_v^o(T_i)}{\int_0^{+\infty} \varepsilon_{iv'} I_{v'}^o(T_i) dv'} dv \quad (33)$$

where $\cos \theta$ stands for $|\vec{u} \cdot \vec{n}_B|$ in the emission term of equation (4). Moreover, the polar angle θ varies from 0 to $\pi/2$.

Identifications of equations (31) and (33) with equation (32) provide all the PDF that can be substituted in equation (29) in order to determine all the random variables (emission point, angles and wavenumber). For example, the wavenumber ν_n of the n^{th} bundle leaving the volume element i is chosen according to:

$$\int_0^{\nu_n} \eta_{iv} d\nu = R_{\nu_n} \int_0^{+\infty} \eta_{iv'} d\nu' \quad (34)$$

where R_{ν_n} is a random number uniformly drawn in the interval [0;1]. For simple PDF, such as those of the angles, analytical integration can be performed leading to inverse relations $X_n = g(R_{X_n})$. For a volume element, the two angles of the n^{th} bundle leaving the volume element are given by:

$$\cos \theta_n = 1 - 2R_{\theta_n} \quad (35)$$

$$\varphi_n = 2\pi R_{\varphi_n} \quad (36)$$

For a diffuse surface element, equation (36) remains suitable while equation (35) becomes:

$$\cos \theta_n = \sqrt{R_{\theta_n}} \quad (37)$$

It is worth noticing that, for a surface element, the angles are defined in the local coordinate system of the surface element, with the unit surface normal pointing in its z -direction (i.e., the polar angle is measured from the unit surface normal).

In a scattering medium, we also have to randomly determine the distance traveled by a bundle before a change of direction due to scattering occurs. As exponential attenuation due to absorption is computed all along a bundle path, the probability for a bundle to be scattered between the distances s and $s + ds$ is:

$$f_{scat}(s) ds = \exp\left[-\int_0^s \sigma_v(s') ds'\right] \sigma_v(s) ds \quad (38)$$

where $f_{scat}(s)$ represents the scattering PDF at location s ($s = 0$ at the emission point and at each scattering location). Substitution of the expression for the scattering PDF into equation (29) gives:

$$\int_0^{\ell_{scat}^{nk}} \sigma_{\nu_n}(s) ds = -\ln(R_{scat}^{nk}) \quad (39)$$

where ℓ_{scat}^{nk} is the distance traveled by the n^{th} bundle between the $(k-1)^{\text{th}}$ and k^{th} scattering events and R_{scat}^{nk} a random number uniformly drawn in the interval [0;1].

In the case of isotropic scattering, equations (35) and (36) can be applied to determine the angles of scattering direction, while in an anisotropic scattering medium, these angles are obtained from the following relations:

$$\int_0^{\theta_s^{nk}} \int_0^{\varphi_s^{nk}} \Phi_{j\nu_n}(\theta, \varphi, \theta', \varphi') \sin \theta' d\theta' d\varphi' = R_{\varphi_s^{nk}} \int_0^{2\pi} \int_0^{\pi} \Phi_{j\nu_n}(\theta, \varphi, \theta', \varphi') \sin \theta' d\theta' d\varphi' = 4\pi R_{\varphi_s^{nk}} \quad (40)$$

$$\int_0^{\theta_s^{nk}} \int_0^{\varphi_s^{nk}} \Phi_{j\nu_n}(\theta, \varphi, \theta', \varphi') \sin \theta' d\theta' d\varphi' = 4\pi R_{\theta_s^{nk}} \quad (41)$$

$\Phi_{j\nu_n}(\theta, \varphi, \theta', \varphi')$ is the spectral scattering phase function in the volume element j containing the k^{th} scattering point of the n^{th} bundle. θ and φ are the angles characterizing the propagation direction before scattering occurs. It is worth noticing that the angles of scattering direction θ_s^{nk} and φ_s^{nk} given by equations (40) and (41) are defined in a local coordinate system having its origin at the scattering point and its z -direction unit vector equal to the unit direction vector of the bundle before scattering occurs (i.e., θ_s^{nk} is measured from the unit direction vector of the bundle before scattering occurs).

In order to control computation convergence, it is possible to subdivide a calculation into Q sub-calculations. For example, if 10^8 bundles are followed, a mean radiative power \bar{P}^R is calculated with all these bundles, and $Q = 100$ sub-means P_1, P_2, \dots, P_Q are calculated with 10^6 bundles each. Then, the variance γ^2 of the mean radiative power \bar{P}^R is:

$$\gamma^2 = \frac{1}{Q-1} \left[\sum_{k=1}^Q (P_k - \bar{P}^R)^2 \right] = \frac{1}{Q-1} \left[\sum_{k=1}^Q P_k^2 - \frac{1}{Q} \left(\sum_{k=1}^Q P_k \right)^2 \right] \quad (42)$$

Using the central limit theorem it can be shown that to reduce the standard deviation by half the total number of bundles has to be quadrupled, leading to quadrupled computation time.

This technique of subdivision into sub-calculations is very convenient for parallelization. Indeed, as the sub-calculations are all independent, they can be easily distributed on computer cores. Moreover, this leads to a parallelization efficiency close to 100% because there is no communication needed between parallel cores during bundle history generation. However, memory storage problems may be encountered when the mesh is composed of a very large number of cells because each computer core has to deal with the whole computation domain.

Discrete ordinates method

The Discrete Ordinates Method (DOM) is based on a discrete representation of the directional variation of the radiative intensity. Thus, the differential form of the Radiative Transfer Equation (RTE, see equation (6)) is replaced by a system of partial differential equations (one equation for each ordinate direction) and integrals over a range of solid angles are approximated by weighted sums over the ordinate directions within that range. Gaussian quadratures called level symmetric or S_N quadratures are often used. That is why DOM is also called the S_N method. N is an even number that indicates the order

of the solution. In a three-dimensional problem, $N_d = N(N + 2)$ discrete ordinates directions are considered.

So the RTE is replaced by a set of N_d equations. The equation corresponding to the m -direction is written as:

$$\begin{aligned} \vec{u}_m \cdot \vec{\nabla} I(s, m) = \eta_v(s) - (\kappa_v(s) + \sigma_v(s)) I_v(s, m) \\ + \frac{\sigma_v(s)}{4\pi} \sum_{j=1}^{N_d} w_j I_v(s, j) \Phi_v(s, j, m) \end{aligned} \quad (43)$$

where the w_j are the quadrature weights associated with the directions \vec{u}_j or j . Equations (43) need boundary conditions, giving the intensities leaving the wall in each direction m , to be solved. For a diffuse surface, the monochromatic intensity $I_v(B_0, m)$ leaving the wall at point B_0 in direction m (such as $\vec{u}_m \cdot \vec{n}_{B_0} > 0$, where \vec{n}_{B_0} is the unit surface normal at the point B_0 , pointing away from surface into the medium) can be expressed as:

$$\begin{aligned} I_v(B_0, m) = \varepsilon_v(B_0) I_v^o(T_{B_0}) \\ + \frac{1 - \varepsilon_v(B_0)}{\pi} \sum_{j \substack{(N_d/2 \text{ values}) \\ \vec{u}_j \cdot \vec{n}_{B_0} < 0}} w_j I_v(B_0, j) |\vec{u}_j \cdot \vec{n}_{B_0}| \end{aligned} \quad (44)$$

Equations (43) and their corresponding boundary conditions (44) show that the intensity in direction m depends on the intensities in all the directions j when wall reflection or scattering is present. Therefore, in these cases, an iterative procedure is needed to compute all the intensities.

Since the unit direction vector \vec{u}_m is independent of the space coordinates, the left-hand side term of equation (43) can be written as:

$$\vec{u}_m \cdot \vec{\nabla} I_v(s, m) = \text{div}(I_v(s, m) \vec{u}_m) \quad (45)$$

Consider an enclosure filled by a non-isothermal, heterogeneous, absorbing, emitting and scattering medium and discretized into volume and surface elements. Each element is assumed to be isothermal and homogeneous and the radiative properties, except the phase function, are assumed to be isotropic.

To set up the numerical solution, a control volume technique, such as the one used in fluid mechanics problems, is applied to equations (43). By substituting equation (45) into equation (43), integrating it over a volume element V_i and using the divergence theorem, equation (43) becomes:

$$\begin{aligned} \sum_{f=1}^{N_i^{\text{faces}}} -\vec{u}_m \cdot \vec{n}_f A_f I_v(f, m) = \\ \left[\eta_{iv} - (\kappa_{iv} + \sigma_{iv}) I_v(C_i, m) + \frac{\sigma_{iv}}{4\pi} \sum_{j=1}^{N_d} w_j I_v(C_i, j) \Phi_{iv}(j, m) \right] V_i \end{aligned} \quad (46)$$

where N_i^{faces} is the number of faces constituting the envelope of the volume V_i , \vec{n}_f the inward surface normal of the face f (pointing

away from the face f into the volume V_i), A_f the area of the face f , $I_v(f, m)$ the monochromatic intensity on the face f in direction m , C_i the center of the volume V_i and $I_v(C_i, m)$ the monochromatic intensity at point C_i in direction m . To obtain equation (46) the assumption has to be made that the intensities $I_v(f, m)$ and $I_v(C_i, m)$ are constant over the area A_f and the volume V_i respectively.

In order to reduce the number of unknowns in equation (46) a spatial differencing scheme is used to express the face intensities as a function of the volume intensities. The step scheme is chosen for its simplicity and robustness. With this spatial differencing scheme, the face intensities are given by the following relations:

- if $\vec{u}_m \cdot \vec{n}_f < 0$, $I_v(f, m) = I_v(C_i, m)$
- if $\vec{u}_m \cdot \vec{n}_f > 0$, either $I_v(f, m) = I_v(C_{if}, m)$ or $I_v(f, m)$ is given by relation (44) if the face f is a boundary.

C_{if} is the center of the volume element that has the face f in common with the volume element V_i . Use of the step scheme in equation (46) leads to:

$$\begin{aligned} I_v(C_i, m) = \\ \frac{\sum_{\substack{f \\ \vec{u}_m \cdot \vec{n}_f > 0}} |\vec{u}_m \cdot \vec{n}_f| A_f I_v(C_{if}, m) + \left[\eta_{iv} + \frac{\sigma_{iv}}{4\pi} \sum_{j=1}^{N_d} w_j I_v(C_i, j) \Phi_{iv}(j, m) \right] V_i}{(\kappa_{iv} + \sigma_{iv}) V_i + \sum_{\substack{f \\ \vec{u}_m \cdot \vec{n}_f < 0}} |\vec{u}_m \cdot \vec{n}_f| A_f} \end{aligned} \quad (47)$$

An iterative procedure, based on a Gauss-Seidel algorithm, is used to compute, for each wavenumber, all the directional intensities defined at all the element centers (volumes and surfaces). Once these intensities have been determined, it is possible to calculate the radiative flux and power with the following relations:

$$\begin{aligned} \phi^R(B_0) = \int_0^{+\infty} \varepsilon_v(B_0) \sum_{\substack{j \substack{(N_d/2 \text{ values}) \\ \vec{u}_j \cdot \vec{n}_{B_0} < 0}}} w_j I_v(B_0, j) |\vec{u}_j \cdot \vec{n}_{B_0}| dv \\ - \pi \int_0^{+\infty} \varepsilon_v(B_0) I_v^o(T_{B_0}) dv \end{aligned} \quad (48)$$

$$P^R(C_i) = \int_0^{+\infty} \kappa_{iv} \sum_{j=1}^{N_d} w_j I_v(C_i, j) dv - 4\pi \int_0^{+\infty} \eta_{iv} dv \quad (49)$$

Gas radiative property models

Absorption/emission spectra of gases have significant spectral dynamics, changing to a considerable degree with thermophysical conditions. For example, figure 1 shows absorption spectra at high resolutions of CO_2 species (on the left, $x_{CO_2} = 0.02$ and $x_{N_2} = 0.98$) and air plasma (on the right) for different temperatures at atmospheric pressure.

If radiative properties can be calculated beforehand at high resolution and for each set of thermochemical conditions encountered, radiative transfer can be accurately computed by using the line-by-line (LBL) approach. With this approach, radiative transfer problems could be solved directly considering the relations given in the two previous parts. However, the LBL approach, which consists in solving the RTE for each wavenumber (several millions of spectral points in general), requires too much CPU time and memory storage for industrial applications. To simplify the RTE resolution and radiative property calculation approximate models at low resolution are generally used. Nevertheless, these models have to take spectral correlation effects into account due to the gas spectra line structure (see Box 2).

In the literature two kinds of approximate models are usually used: global models and band models. Global models, such as the Weighted Sum of Gray Gases (WSGG) [14], the Spectral Line-based Weighted sum of gray gases (SLW) [7] or the Absorption Distribution Function (ADF) [26], allow the direct solution of the RTE with radiative properties relative to the whole spectrum. These models are accurate and convenient for uniform media but it becomes difficult to define the parameters of these models for non-uniform gaseous mixtures. In addition, global models are incompatible with the treatment of particles or non-gray walls. Band models are generally more accurate but more costly in terms of computational resources. In this modeling the spectrum is subdivided into bands and radiative properties are averaged over each spectral band. Under LTE conditions, to minimize spectral correlation problems, the bands have to be sufficiently narrow to consider the Planck function constant over each band for all considered temperatures (this can be explained by the fact that, when equation (6) or (7) is averaged over a spectral band, the average of the product of a radiative quantity with the Planck function can be considered equal to the product of the averages if the Planck function is almost constant over each spectral band). Several band models for gas radiative properties exist in the literature, but only band models, used in the radiation solvers developed at Onera (REA and ASTRE), are presented in the following sections.

The first two sections are dedicated to two well-known band models which are used to take into account spectral dynamics in radiative transfer problems: the Correlated-K (CK) model and one type of Statistical Narrow Band (SNB) model. The former, which is formulated in terms of the absorption coefficient, is appropriate for solving the two RTE formulations described in the first part, while the latter, formulated in terms of mean transmissivity, is only suitable for RTE formulation in terms of transmissivity. In the last section, the basic box model is presented. This simplified model can be used when spectral correlation effects can be neglected. For each model, cases of uniform and non-uniform media are discussed, as well as the case of media composed of several radiating species.

Correlated-k (CK) model

Uniform media

To compute average radiative properties, as, for example, transmissivities, knowledge of spectral band line positions is not necessary. Knowledge of the distribution function of the absorption coefficient is sufficient. This is the idea on which the CK model, initially used for atmospheric applications [13], is based. The cumulative distribution function used is defined by:

$$g(k) = \frac{1}{\Delta\nu} \int_{\nu \in \Delta\nu / k_\nu \leq k} d\nu \quad (50)$$

for $k \in [k_{\min}; k_{\max}]$, where k_{\min} and k_{\max} are the extreme values, reached in the spectral band $\Delta\nu$, of the reduced monochromatic absorption coefficient k_ν , defined as the ratio κ_ν / xp . Mean transmissivity of a uniform column of length l can be expressed with the function g :

$$\bar{\tau}^{\Delta\nu}(l) = \frac{1}{\Delta\nu} \int_{\Delta\nu} \exp(-xplk_\nu) d\nu = \int_{k_{\min}}^{k_{\max}} \exp(-xplk) \frac{\partial g}{\partial k} dk \quad (51)$$

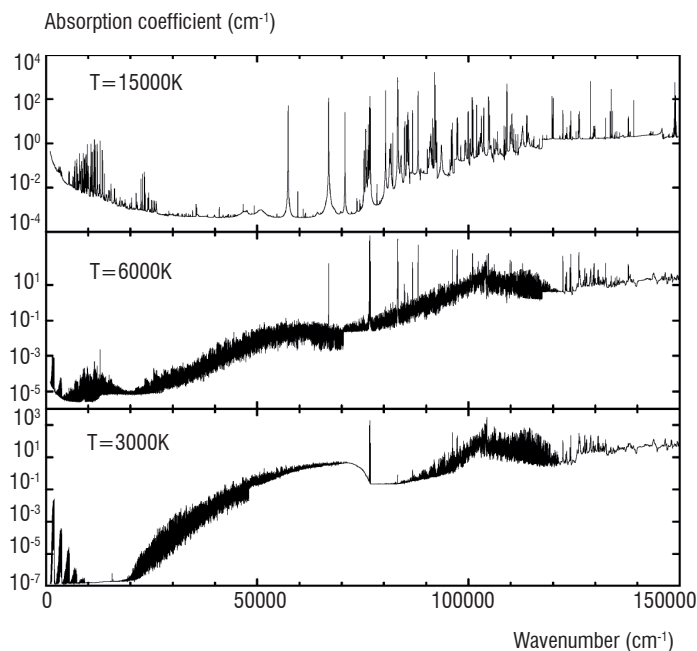
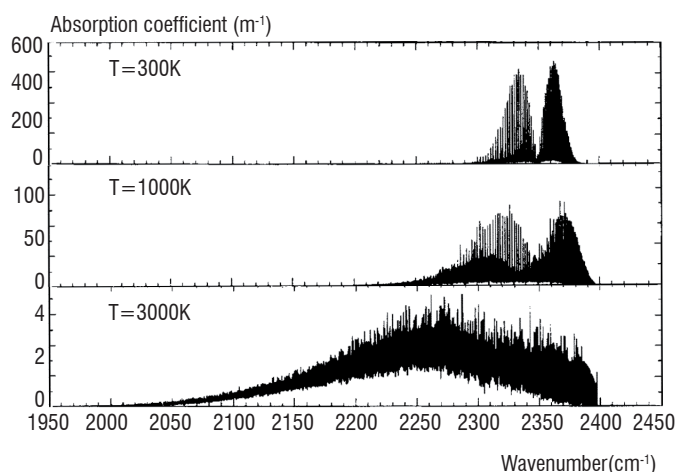


Figure 1 - Absorption spectra of CO_2 species (on the left – extracted from Ref. [34]) and air plasma (on the right – extracted from Ref. [3]) at atmospheric pressure for different temperatures.

Box 2 - Spectral correlation phenomenon

The phenomenon of spectral correlation is due to the spectral dynamics of emission and absorption spectra and the fact that emission is spectrally located at the same position as absorption. The following simple example demonstrates the importance of this phenomenon in radiative transfer problems where integrated values are usually wanted.

Consider two columns 1 and 2, characterized respectively by an emissivity ε_ν and a transmissivity τ_ν (see figure B2-01) of two spectral lines (crudely represented by two crenels) located in a spectral interval $\Delta\nu$. The monochromatic intensity emitted by column 1 and transmitted by column 2 can be expressed as $I_\nu = I_\nu^\circ(T_1)\varepsilon_\nu\tau_\nu$, where T_1 is the temperature of column 1. To simplify, $I_\nu^\circ(T_1)$ is assumed to be constant over the spectral band $\Delta\nu$ and equal to $I_{\nu_c}^\circ(T_1)$ where ν_c is the center of the band $\Delta\nu$. The intensity averaged over the band $\Delta\nu$ is then written:

$$\bar{I}^{\Delta\nu} = I_{\nu_c}^\circ(T_1) \frac{1}{\Delta\nu} \int_{\nu_c - \Delta\nu/2}^{\nu_c + \Delta\nu/2} \varepsilon_\nu \tau_\nu d\nu = 0 \quad (II-1)$$

This intensity is equal to zero because the product $\varepsilon_\nu \tau_\nu$ is equal to zero for any wavenumber included in the spectral band $\Delta\nu$. Indeed, emission by column 1 is located exactly at the same spectral positions where absorption in column 2 occurs. This result takes spectral correlations entirely into account. As real spectra do not have a structure as simple as those described in figure B2-01 another approach to calculate this mean intensity would be to not consider spectral correlations but to use the mean values of emissivity and transmissivity of the two columns. The result is:

$$\bar{I}^{\Delta\nu} = I_{\nu_c}^\circ(T_1) \bar{\varepsilon}^{\Delta\nu} \bar{\tau}^{\Delta\nu} = I_{\nu_c}^\circ(T_1) \frac{1}{\Delta\nu} \int_{\nu_c - \Delta\nu/2}^{\nu_c + \Delta\nu/2} \varepsilon_\nu d\nu \times \frac{1}{\Delta\nu} \int_{\nu_c - \Delta\nu/2}^{\nu_c + \Delta\nu/2} \tau_\nu d\nu = \frac{2}{9} I_{\nu_c}^\circ(T_1) \quad (II-2)$$

which gives a result totally different from relation (II-1), both quantitatively and qualitatively.

This is a simple example but it is a good illustration of how not accounting for spectral correlations between emission and absorption terms can lead to absurd results. As explained in the section "Gas radiative property models", spectral correlation effects can be more or less significant depending on the type of application.

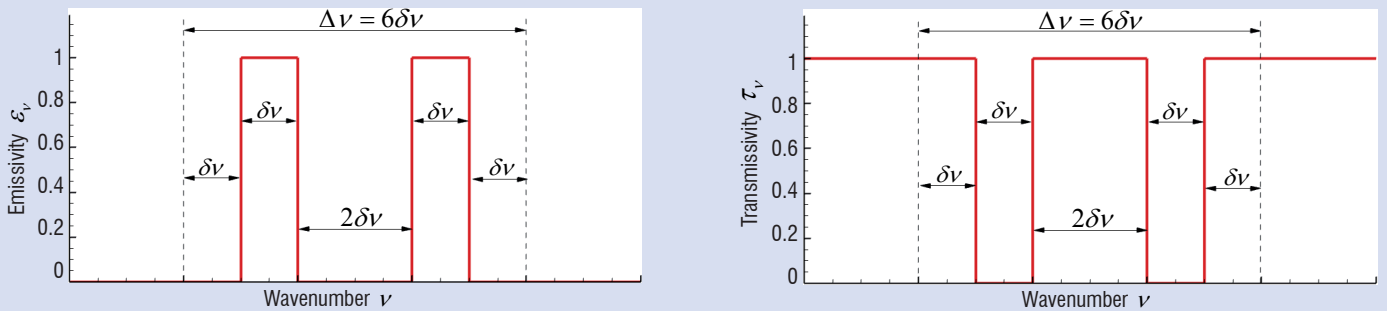


Figure B2-01- Emissivity of column 1 (on the left) and transmissivity of column 2 (on the right).

where x is the molar fraction of the absorbing species and p the pressure in the column. The function $\partial g / \partial k$ represents the inverse Laplace transform of $\bar{\tau}^{\Delta\nu}(l)$. By introducing the inverse function of $g, G \rightarrow k(G)$, relation (51) can be written:

$$\bar{\tau}^{\Delta\nu}(l) = \int_0^1 \exp(-xplk(G)) dG \quad (52)$$

In fact, $k(G)$ is the absorption coefficient reordered vs the wavenumber scaled by $dG = d\nu / \Delta\nu$, as shown in figure 2. It is convenient to use this function because $k(G)$ is monotonous and increasing, inversely as the function $\nu \rightarrow k_\nu$, which has significant spectral dynamics. Therefore, integration in relation (52) can be achieved using quadrature with a small number of points (about ten usually):

$$\bar{\tau}^{\Delta\nu}(l) = \sum_{i=1}^n w_i \exp(-xplk(G_i)) \quad (53)$$

where n, G_i and w_i are the quadrature order, points and weights respectively.

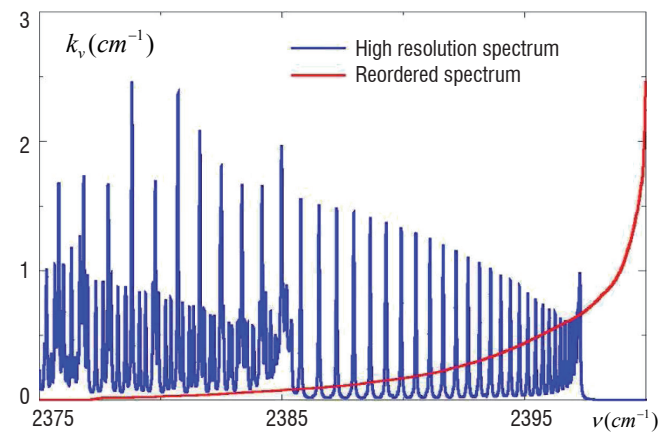


Figure 2 - Example of a reordered spectrum on a spectral band [29].

Non-uniform media

This model is extended to non-uniform media by assuming that the rearrangement function $\nu \rightarrow G$ is spatially independent. This assumption on spectral correlations allows association of the reordered absorption coefficients for different thermophysical conditions. Therefore, the mean transmissivity of an inhomogeneous column is approximated by:

$$\bar{\tau}^{\Delta\nu}(l) = \sum_{i=1}^n w_i \exp\left[-\int_0^l x(s)p(s)k(G_i, s)ds\right] \quad (54)$$

The weights w_i and the values $k(G_i, s)$ for each narrow band are the CK model parameters. In practical cases, the values $k(G_i, s)$ depend on temperature, pressure and the gas mixture composition. This method, based on the reordering of the absorption coefficient to express the mean transmissivity, can be also used for any radiative quantities that depend on κ_ν , such as the mean radiative intensity at any point M of abscissa s :

$$\bar{I}^{\Delta\nu}(s) = \sum_{i=1}^n w_i I_{G_i}(s) \quad (55)$$

where $I_{G_i}(s)$ is the pseudo-monochromatic intensity at the point M at the pseudo wavenumber G_i . This intensity satisfies, for each quadrature point, the following RTE formulation (given here at LTE conditions without scattering):

$$\frac{\partial I_{G_i}(s)}{\partial s} = x(s)p(s)k(G_i, s)\left[\bar{I}^{\Delta\nu}(s) - I_{G_i}(s)\right] \quad (56)$$

When two species A and B may absorb in the same spectral band, the following approximation:

$$\bar{\tau}^{\Delta\nu}(l) = \bar{\tau}_A^{\Delta\nu}(l) \times \bar{\tau}_B^{\Delta\nu}(l) \quad (57)$$

can be used with a good degree of accuracy since there is no physical reason to have significant correlations between the spectra of different species. Thereby, the mean transmissivities $\bar{\tau}_A^{\Delta\nu}$ and $\bar{\tau}_B^{\Delta\nu}$ are calculated with relation (54), leading to:

$$\begin{aligned} \bar{\tau}^{\Delta\nu}(l) &= \sum_{i=1}^n w_i \exp\left[-\int_0^l x_A(s)p(s)k_A(G_i, s)ds\right] \\ &\quad \times \sum_{i=1}^n w_i \exp\left[-\int_0^l x_B(s)p(s)k_B(G_i, s)ds\right] \\ &= \sum_{i=1}^n \sum_{j=1}^n w_i w_j \exp\left[-\int_0^l \left(x_A(s)p(s)k_A(G_i, s) + x_B(s)p(s)k_B(G_j, s)\right)ds\right] \end{aligned} \quad (58)$$

The latter expression can be interpreted as the use of an N^2 -point quadrature with the weights $w_i w_j$. The average intensity is given by the following relation:

$$\bar{I}^{\Delta\nu}(s) = \sum_{i=1}^n \sum_{j=1}^n w_i w_j I_{G_i G_j}(s) \quad (59)$$

where each intensity $I_{G_i G_j}(s)$ satisfies the following RTE formulation (given here at LTE conditions without scattering):

$$\begin{aligned} \frac{\partial I_{G_i G_j}(s)}{\partial s} &= \left(x_A(s)p(s)k_A(G_i, s) + x_B(s)p(s)k_B(G_j, s)\right) \\ &\quad \times \left[\bar{I}^{\Delta\nu}(s) - I_{G_i G_j}(s)\right] \end{aligned} \quad (60)$$

These relations can easily be extended to m absorbing species considering an N^m -point quadrature.

Statistical Narrow Band (SNB) model

Uniform media

Another band model group is the family of Statistical Narrow Band (SNB) models. The random SNB model of Mayer and Goody [13] has been chosen for the applications studied at Onera. This model is based on statistical assumptions for line positions and intensities within a narrow band of width $\Delta\nu$, allowing the transmissivity of a uniform column of length l , averaged over $\Delta\nu$, to be expressed as:

$$\bar{\tau}^{\Delta\nu}(l) = \frac{1}{\Delta\nu} \int_{\Delta\nu} \exp(-xpl\kappa_\nu) d\nu = \exp\left(-\frac{\bar{W}}{\delta}\right) \quad (61)$$

where $\delta = \Delta\nu / N$ is the mean spacing between the N line positions within $\Delta\nu$, and \bar{W} is the mean black equivalent line width of these lines, defined as:

$$\bar{W} = \frac{1}{N} \sum_{r=1}^N \int_{-\infty}^{+\infty} [1 - \exp(-\kappa_r^r l)] d\nu \quad (62)$$

where κ_r^r is the contribution of the r^{th} line to the absorption coefficient. Many analytical expressions for \bar{W} / δ have been proposed in the literature by assuming: (i) a suitable probability distribution function (PDF) $P(S)$ of line intensities (of the PDF usually used, the uniform distribution, the Goody exponential distribution and the Malkmus tailed inverse-exponential distribution can be mentioned), (ii) a unique spectral line shape for all lines, Gaussian (to characterize the Doppler broadening effect) or Lorentzian (to characterize the collisional broadening effect), with a constant half-width at half-maximum (HWHM) γ_0^D or γ_0^L . All analytical expressions of \bar{W} / δ , summarized in Ref. [34], actually depend on only two parameters, \bar{k} and $\bar{\beta}$. The first of these, \bar{k} , can be identified with a reduced mean absorption coefficient and is always related to the mean line intensity $\bar{S} = \int SP(S)dS$ by the relation $\bar{k} = \bar{S} / \delta$. The second, $\bar{\beta}$, characterizes the degree of line overlapping and is always proportional to the ratio $\gamma_0^{L/D} / \delta$ (L/D stands for 'Lorentz' or 'Doppler'). The parameter $\bar{\beta}$ can be generated from a spectroscopic database or from curve fitting. In the latter method the analytical expression $\bar{W}_{L/D} / \delta$ is fitted to the curve of growth (defined as the opposite of the logarithm of the mean transmissivity versus the column length l), obtained with line by line calculation.

Under some thermophysical conditions the lines have a Voigt profile, for which there is no analytical expression of the mean black equivalent line width \bar{W}_V . Several approximations of \bar{W}_V , based on expressions of \bar{W}_L and \bar{W}_D , for Lorentz and Doppler regimes respectively, can be used. The expression of Ludwig [20] is generally an accurate approximation:

$$\frac{\bar{W}_V}{\delta} = xpl\bar{k} \sqrt{1 - \Omega^{-1/2}} \quad (63)$$

with:

$$\Omega = \left[1 - \left(\frac{1}{xpl\bar{k}} \frac{\bar{W}_D}{\delta}\right)^2\right]^{-2} + \left[1 - \left(\frac{1}{xpl\bar{k}} \frac{\bar{W}_L}{\delta}\right)^2\right]^{-2} - 1 \quad (64)$$

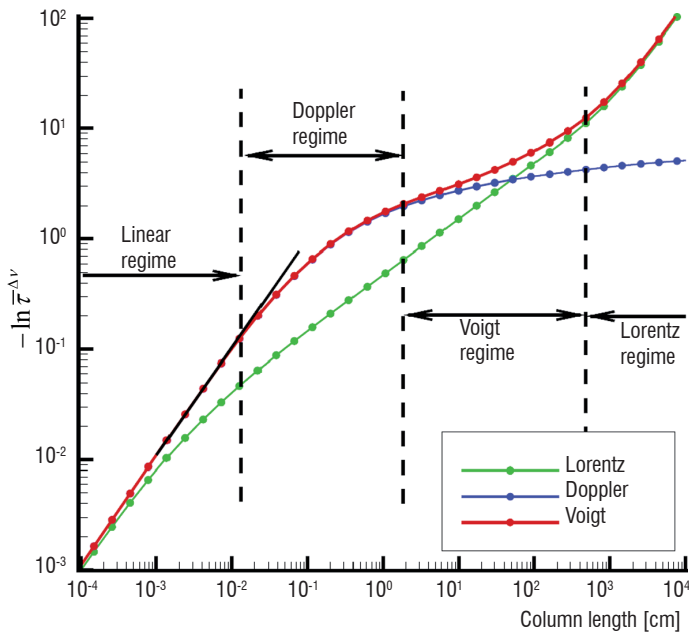


Figure 3 - Typical curve of growth depending on the broadening regime [17].

Figure 3 shows an example of the typical curve of growth for a spectral band of 1000 cm^{-1} ($112000\text{--}113000 \text{ cm}^{-1}$) for the N_2 Birge-Hopfield system at atmospheric pressure and 8000 K . The different broadening regimes, like Doppler and Lorentzian regimes, are indicated in figure 3. The parameters β_D and β_L are adjusted to fit expression (63) to the curve of growth.

Non-uniform media

Different approximations exist in the literature allowing the extension of SNB models to the case of non-uniform gaseous columns. An extensive review of these approximations is given by Young [39]. The classic Curtis-Godson (CG) approximation used in practical cases is briefly presented here.

The main assumption of CG approximations is that the curves of growth of a non-uniform column versus the optical path $u = \int_0^l x(s)p(s)ds$ have the same behavior as those obtained for uniform columns. Therefore, mean transmissivity is written:

$$\bar{\tau}^{\Delta\nu}(l) = \exp\left(-\frac{\overline{W_V^*}}{\delta}\right) \quad (65)$$

where $\overline{W_V^*}/\delta$ is given by equations (63) and (64), in which the product xpk is replaced by:

$$\overline{k^*u} = \int_0^l x(s)p(s)\overline{k(s)}ds \quad (66)$$

Moreover, the terms $\overline{W_L}/\delta$ and $\overline{W_D}/\delta$ in equation (64) are replaced, respectively, by $\overline{W_L^*}/\delta$ and $\overline{W_D^*}/\delta$, which are calculated with the same analytical formulations as those used for a uniform column, but with k^* and $\beta_{L/D}^*$ instead of \overline{k} and $\overline{\beta_{L/D}}$. With the classic CG approximation, $\beta_{L/D}^*$ is expressed as:

$$\beta_{L/D}^* = \frac{1}{\overline{k^*u}} \int_0^l x(s)p(s)\overline{k(s)}\overline{\beta_{L/D}(s)}ds \quad (67)$$

The “*” parameters are consequently obtained from parameters calculated for uniform media.

If two species A and B absorb in the same spectral band, the approximation given by equation (57) can be used.

Box model

In some applications, the spectral correlation effect on radiative transfer can be weak. This is the case, for example, when the medium is optically thin or when the absorption spectrum has weak spectral dynamics. The latter case is illustrated in figure 4 which shows spectral emissivities of two $\text{H}_2\text{O}-\text{N}_2$ mixture columns at two different pressures but with the same optical path (xpl product). The collision broadening effect leads to smooth radiative properties at high pressure in such a way that the spectral dynamics become weaker.

In these situations, information on the spectral distribution (distribution function for the CK model, overlapping parameter β for the SNB model) can be ignored and the model parameter is only the reduced absorption coefficient \overline{k} (box model parameter).

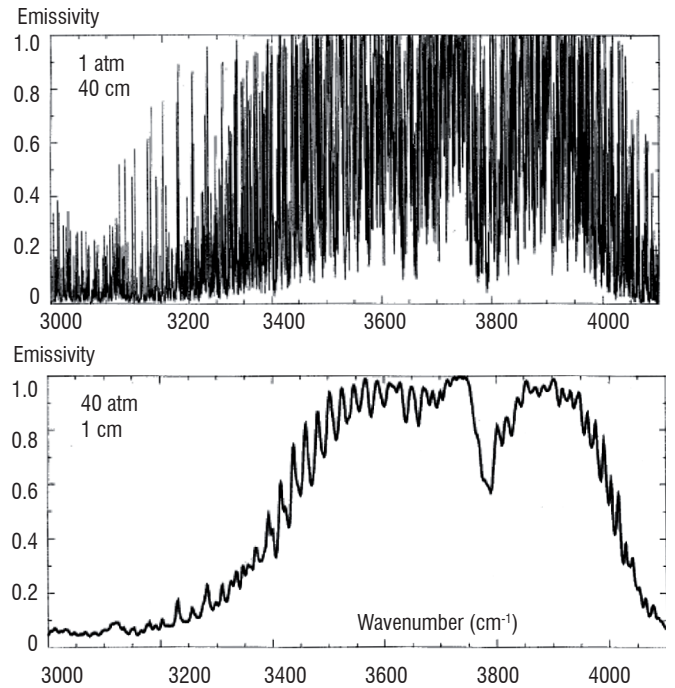


Figure 4 - Emissivity spectra of two $\text{H}_2\text{O}-\text{N}_2$ mixture ($x_{\text{H}_2\text{O}} = 0.5$) columns at 800 K as a function of pressure condition at a constant product xpl [34].

If the integral form of the RTE (see equation (7)) is used then the transmissivity, averaged over $\Delta\nu$, of a uniform column of length l can be expressed to a good approximation as:

$$\bar{\tau}^{\Delta\nu}(l) = \exp(-xpk\overline{l}) \quad (68)$$

For non-uniform media the following relation is simply used:

$$\bar{\tau}^{\Delta\nu}(l) = \exp\left(-\int_0^l x(s)p(s)\overline{k(s)}ds\right) \quad (69)$$

and for mixture media, a relation quite similar to equation (57) can be used.

Radiative property models of particles

When a photon interacts with a medium containing small particles, the radiative intensity may be changed by absorption and/or scattering. This situation is mostly encountered in a combustion engine where soot or alumina particles are present.

This part of the paper only deals with radiative properties of spherical particles, since particles are assumed to be spherical in the applications studied at Onera. Moreover, scattering is considered as independent. In this situation, the radiative properties of a cloud of spherical particles of radius r , interacting with an incident radiation of wavenumber ν , are governed by only two independent non-dimensional parameters [23]:

- complex index of refraction of the particles:

$$m(s, \nu) = n(s, \nu) - ik(s, \nu),$$
- size parameter (also called the Mie parameter): $x = 2\pi r\nu$.

Note that the complex index m is a function of wavenumber and local thermophysical conditions at the point of abscissa s .

When the size parameter is not very small or very large compared to unity, the radiative properties are usually determined from the Mie theory, a general theory describing interaction between an electromagnetic wave and a spherical particle. In other cases, this theory can be simplified: the Rayleigh theory (for $x \ll 1$) and geometric optics (for $x \gg 1$) are recovered. The case $x \ll 1$ is, in particular, discussed in the third section.

Radiative property expressions

From a general point of view, the absorption (or scattering) phenomenon is quantified by an efficiency factor Q_{abs} (or Q_{sca}) which is defined as the ratio between the absorption (or scattering) cross section and the actual surface particle πr^2 . The Mie theory gives analytical expressions [1] to calculate these efficiencies for an isolated particle, assumed to be spherical, homogeneous and isothermal. The expressions depend on the local complex index of refraction of the particle and the Mie parameter. Figure 5 shows typical changes in the efficiency coefficients as a function of the Mie parameter for alumina particles.

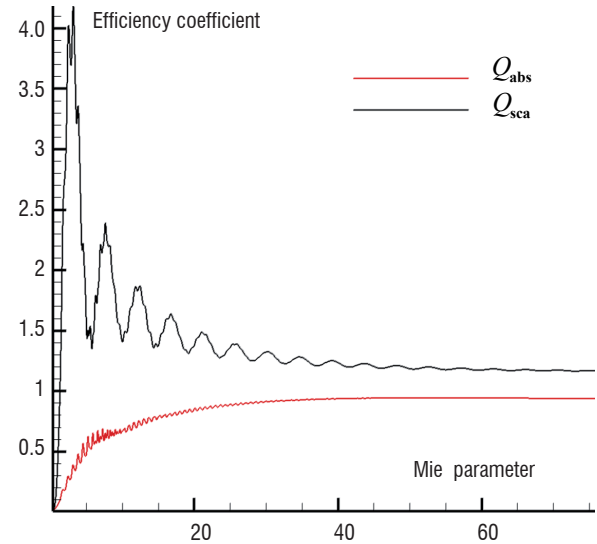


Figure 5 - Absorption and scattering efficiency coefficients for alumina particles ($m = 1.7 - 2.10^{-3}i$).

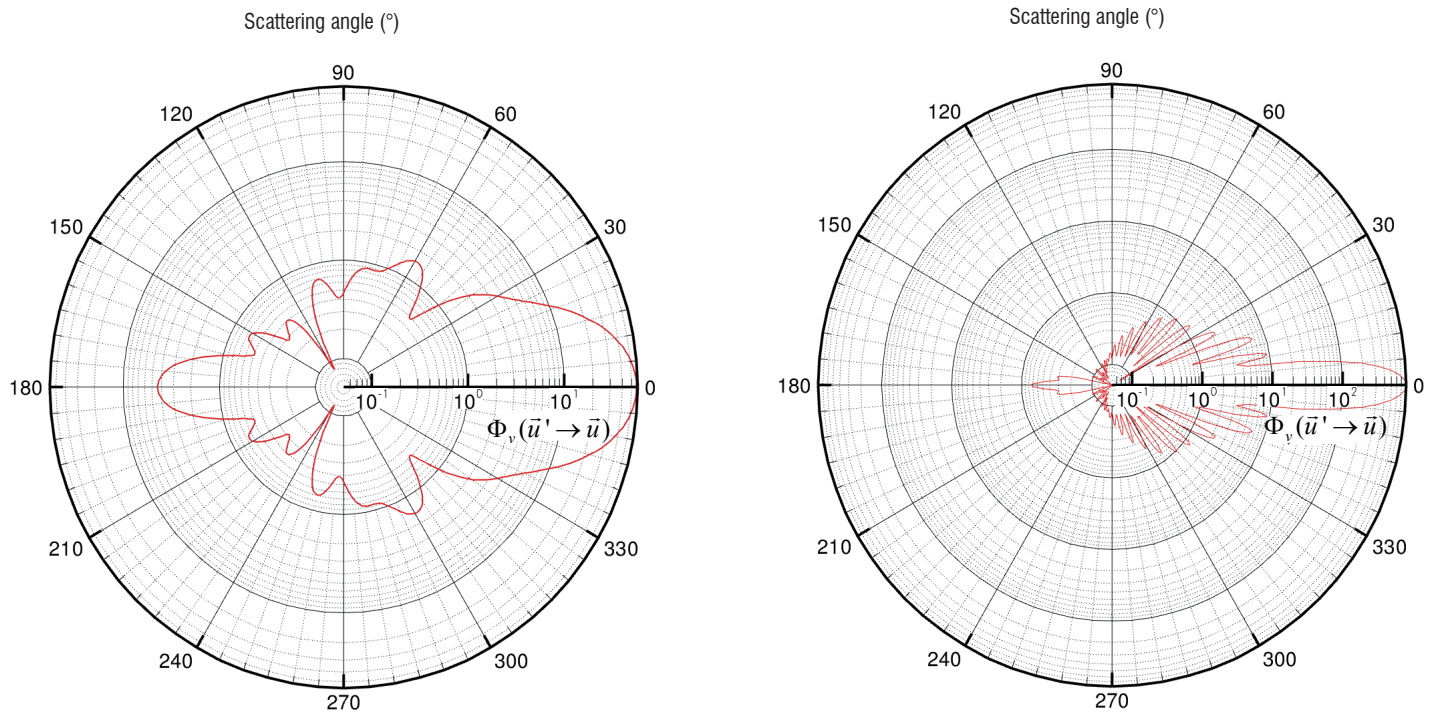


Figure 6 - Polar plots of the scattering phase function for a single alumina particle ($m = 1.7 - 2.10^{-3}i$) with $\nu = 10000 \text{ cm}^{-1}$ and $r = 1 \text{ }\mu\text{m}$ (on the left), $r = 4 \text{ }\mu\text{m}$ (on the right).

From the efficiencies Q_{abs} and Q_{sca} the absorption and scattering coefficients at the point of abscissa s can be obtained for a cloud of particles of non-uniform size:

$$\kappa_v(s) = \int_0^\infty \frac{3}{4} \frac{Q_{abs}(m(s), r, \nu)}{r} f_V(r, s) dr \quad (70)$$

$$\sigma_v(s) = \int_0^\infty \frac{3}{4} \frac{Q_{sca}(m(s), r, \nu)}{r} f_V(r, s) dr \quad (71)$$

where $f_V(r, s) dr$ is the volume fraction, at the abscissa s , of the particles having a radius between r and $r + dr$.

To characterize anisotropic scattering due to particles, the scattering phase function is required. Its expression is:

$$\Phi_v(s, \vec{u}' \rightarrow \vec{u}) = \frac{1}{\sigma_v(s)} \int_0^\infty \frac{3}{4} \frac{Q_{sca}(m(s), r, \nu)}{r} \Phi_v(s, \vec{u}' \rightarrow \vec{u}, r) f_V(r, s) dr \quad (72)$$

where $\Phi_v(s, \vec{u}' \rightarrow \vec{u}, r)$ is the scattering phase function given by analytical expressions from Mie theory for one size of particle. Figure 6 gives, for example, polar plots of the scattering phase function for two radii of alumina particle at 10000 cm^{-1} .

Radiative property modeling

Since particles are often present simultaneously with gases it is more convenient to consider the same spectral discretization for both. Therefore, particle radiative properties have to be averaged over spectral bands $\Delta\nu$. However, contrary to the case of gas radiation, the spectral dynamics of particle absorption spectra is, in general, sufficiently weak to make the spectral correlations insignificant. In this situation the box model can be used and the model parameters are only the absorption and scattering coefficients and the phase function averaged over each spectral band.

Considering a radius discretization Δr_i , expression (70), for example, becomes:

$$\bar{\kappa}^{\Delta\nu}(s) = \sum_i \frac{1}{\Delta\nu} \int_{\Delta\nu} \int_{\Delta r_i} \frac{3}{4} \frac{Q_{abs}(m(s), r, \nu)}{r} f_V(r, s) dr d\nu \quad (73)$$

If the spectral bands are sufficiently narrow to consider the complex index m to be constant over each spectral band then the double integration can be reduced to only one, over the Mie parameter x [15]:

$$\bar{\kappa}^{\Delta\nu}(s) = \sum_i \frac{3}{4} f_{V,i}(s) \int_{\Delta x_i} \frac{Q_{abs}(m(s), x)}{x} g(x - x_i) dx \quad (74)$$

In this expression, $f_{V,i}(s) \Delta r_i$ is the volume fraction of particles having a radius contained in the interval Δr_i and the Mie parameter x_i is equal to $2\pi r_i \nu_c$ where ν_c is the centre of the band $\Delta\nu$ and r_i the centre of the interval Δr_i . $g(x - x_i)$ is a distribution function describing the variation of x due to a particle size distribution in Δr_i and variation of ν in $\Delta\nu$. Several forms of the g function have been used by various researchers. A modified gamma distribution is generally used. The choice of the parameters characterizing this distribution depends on the type of application.

Similarly, expressions (71) and (72) can be expressed as:

$$\bar{\sigma}^{\Delta\nu}(s) = \sum_i \frac{3}{4} f_{V,i}(s) \int_{\Delta x_i} \frac{Q_{sca}(m(s), x)}{x} g(x - x_i) dx \quad (75)$$

$$\bar{\Phi}^{\Delta\nu}(s, \vec{u}' \rightarrow \vec{u}) = \sum_i \frac{3}{4} \frac{f_{V,i}(s)}{\bar{\sigma}^{\Delta\nu}(s)} \times \int_{\Delta x_i} \frac{Q_{sca}(m(s), x)}{x} \Phi_x(s, \vec{u}' \rightarrow \vec{u}) g(x - x_i) dx \quad (76)$$

If the medium contains several types of particles (each type of particle being characterized by a different complex index of refraction) then the mixture radiative property calculation presents no difficulty because the radiative properties of the particles (absorption and scattering coefficients and phase function) are additive.

Rayleigh scattering regime

If the particles are sufficiently small to assume the Mie parameter x to be very small compared to unity (for instance, primary soot particles or gas molecules satisfy the condition $x \ll 1$), the radiative properties can be easily obtained by considering the appropriate limit of the general Mie equation solution: the Rayleigh scattering regime. In this case the Mie parameter dependences of the efficiencies are: $Q_{abs} \propto x$ and $Q_{sca} \propto x^4$. As $x \ll 1$, scattering can be neglected in comparison to absorption.

In the Rayleigh regime the absorption efficiency is given by a simple analytical formula giving a simple expression for the absorption coefficient [23]:

$$\kappa_v(s) = \frac{36\pi n(s, \nu) k(s, \nu)}{(n^2(s, \nu) - k^2(s, \nu) + 2)^2 + (2n(s, \nu)k(s, \nu))^2} \nu f_V(s) \quad (77)$$

$$= A(s, \nu) \nu f_V(s)$$

where $f_V(s)$ is the local volume fraction of particles and $A(s, \nu)$ a function depending on the real and imaginary parts of the local complex index of the particles. Thus, for sufficiently narrow spectral bands, as previously discussed, the average absorption coefficient is expressed as:

$$\bar{\kappa}^{\Delta\nu}(s) = A(s, \nu_c) \nu_c f_V(s) \quad (78)$$

Available models and typical applications

The development of radiative property models, presented in the two previous parts, requires data such as spectroscopic databases for gases or complex indices of refraction for particles. The following sections give a description of the gas and particle radiative property models, implemented in the radiation solvers (ASTRE and REA) developed at Onera. In particular, the available models for two main applications, radiation in flames (combustion) and radiation in plasmas (atmospheric entry problems), are presented. The majority of gas radiative property models have been developed by the EM2C laboratory or in collaboration with them. In this case, the model development is based on HTGR spectroscopic databases [24].

Radiation in combustion applications

Flames emit, scatter and absorb radiation mainly in the infrared spectral range. The participating medium is in general constituted of combustion gases and particles such as: (i) CO_2 , H_2O , CO molecules, and soot particles, for air breathing combustion (laboratory flames or combustion chamber), (ii) CO_2 , H_2O , CO , HCl molecules, and alumina particles, for aluminized solid propellant combustion.

Air breathing combustion at atmospheric pressure

For atmospheric pressure applications, the spectral dynamics of the gas absorption coefficient is so significant that accurate radiative transfer prediction needs a spectrally correlated model.

For the treatment of CO_2 and H_2O radiation in the infrared spectral range, a CK model is used. Model parameters have been generated by Soufiani and Taine [33] for applications in the 300-2500 K temperature range. A seven-point quadrature has been used (the same for the two species and for all the spectral bands). The pseudo-monochromatic absorption coefficient $k_A(G_i, s)$ is given by the following expression (subscript A represents CO_2 or H_2O species):

$$k_A(G_i, s) = x_A(s) p_{atm} [T(s) Q_A(T(s))]^{-1} k_A^*(G_i, s) \quad (79)$$

where $Q_A(T(s))$ is the partition function of the absorbing molecule at the temperature $T(s)$ at the abscissa s . The parameters $k_A^*(G_i, s)$ are tabulated as a function of T (a set of 16 temperature values). In the case of H_2O they are also tabulated versus x_{H_2O} (a set of 5 values) to take into account the strong dependence of line broadening on the molar fraction x_{H_2O} . The useful wavenumber range (150-9300 cm^{-1}) has been divided into 44 spectral bands with a variable width for H_2O . CO_2 absorbs radiation in only 17 of these bands. For an RTE formulation in terms of transmissivity, the model is constituted of 308 spectral points (44×7) whereas 1022 ($17 \times 7 \times 7 + (44-17) \times 7$) spectral points are necessary for an RTE formulation in terms of the absorption coefficient due to the double quadrature required in the overlapping bands.

In addition, it may be necessary to take soot particle radiation into account but soot particle aggregation is not considered. As primary soot particles are very small spherical particles, expressions valid for the Rayleigh regime can be used and scattering can be neglected. To compute the average absorption coefficient expression (78) has been simplified to the following [35], [37]:

$$\bar{\kappa}^{\Delta\nu}(s) = 5.5\nu_c f_\nu(s) \quad (80)$$

due to lack of information on values, of real and imaginary parts of the soot refraction index, over the whole spectrum and as a function of soot composition and temperature.

For example, the sooty turbulent ethylene jet flame experimentally studied by Coppalle and Joyeux [5] has been simulated [37], [38]. The CK model, for the gas mixture, associated with equation (80), for soot particles, has been used to compute radiative transfer in the flame. Figure 7 shows the TRI effect (see Box 1) on the radiative power field.

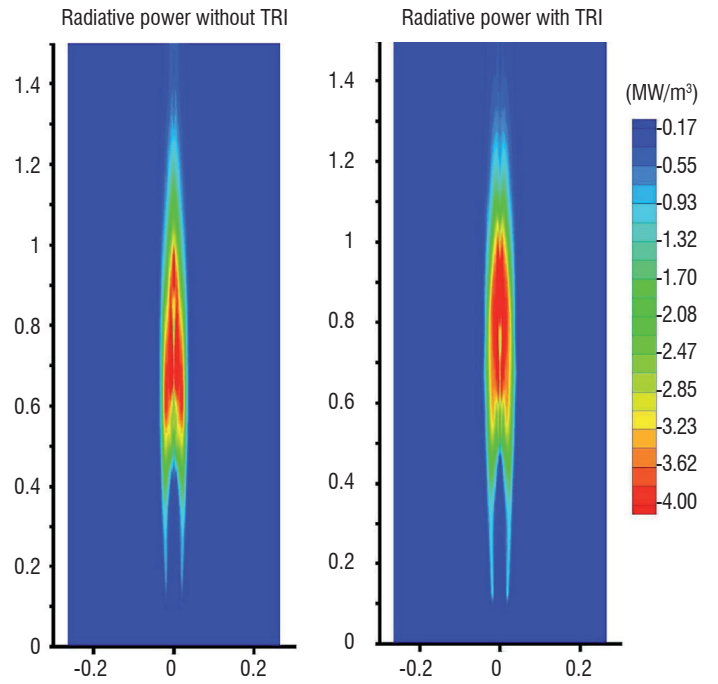


Figure 7 - Radiative power without (on the left) and with (on the right) turbulence-radiation interaction in a sooty turbulent ethylene jet flame [37], [38].

Air breathing combustion at high pressure

At high pressure, due to the collision broadening effect, the absorption spectra display smoother spectral dynamics than those at atmospheric pressure. In this case, the spectral correlation effect is weak and the box model can be used to model the gas radiative properties. Such an approach has been used by Pierrot [25] to deal with CO_2 , H_2O and CO radiation at high pressure in an aeronautical combustion chamber. This model is called the High Pressure Box Model (HPBM). The model parameters are the reduced absorption coefficients $\bar{\kappa}$ which are extracted from the SNB model parameters developed by Soufiani and Taine [33]. The temperature and spectral ranges considered are 700-2500 K and 150-9300 cm^{-1} . The temperature grid is composed of 10 values with a constant step equal to 200 K. The spectral range is divided into 367 bands of constant width equal to 25 cm^{-1} . This model version is called HPBM 367.

To reduce CPU times, Pierrot has enlarged the band width, grouping bands with similar radiative properties. The new model is then constituted of 26 bands (HPBM 26) and gives similar results in terms of accuracy at high pressure.

If the configuration studied produces a significant quantity of soot particles, their radiation can be taken into account in the same way as for combustion at atmospheric pressure (see previous subsection).

Figure 8 shows a typical application result. Radiative transfer has been calculated in a combustion chamber using the HPBM 26 model for CO_2 , H_2O , CO radiation and equation (80) for soot particle radiation. Negative values indicate that local emission is greater than local absorption and vice versa.

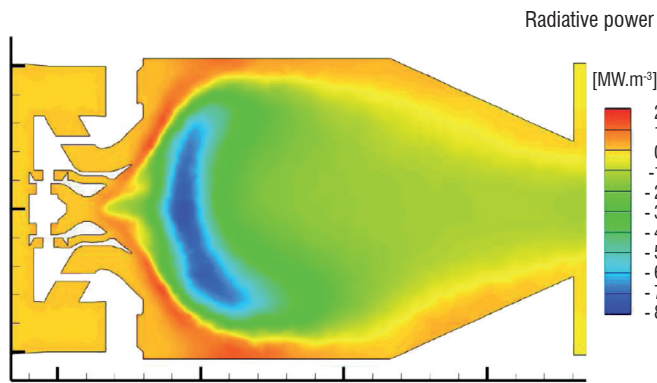


Figure 8 - Radiative power field in a combustion chamber at 10 bar, fitted with a multipoint injector.

Combustion in an aluminized solid propellant rocket engine

In a solid propellant motor, temperatures up to 3600 K, and pressure between 50 to 150 bar, are reached in the combustion chamber. In this situation, radiative transfer in the chamber can be calculated without taking into account spectral correlation, for the same reasons as those given in the previous subsection.

For the gas radiative property model, the box model, developed by Duval [11], with consideration of the CO_2 , H_2O , CO and HCl species, is used. The \bar{k} parameters are tabulated for a 300-3500 K temperature range, and for 43 spectral bands of variable width between 150 and 9300 cm^{-1} .

The radiative properties of alumina particles are calculated using Mie theory. Absorption and scattering coefficients and phase function are computed on the assumption that the distribution function g in equations (74), (75) and (76) is a Gaussian function. In general, several classes of particle sizes are used (typically between one and five samples) to describe particle size distribution. The complex refraction index of alumina is modeled as a function of wavenumber and temperature in accordance with the expressions given by Dombrovsky [9] or Joumani [15].

Radiation in atmospheric (re-)entry applications

Two SNB models for atmospheric (re-)entry applications have been implemented: one for the Martian atmosphere at Local Thermodynamic Equilibrium (LTE) [28], [31] and the other for the Earth's atmosphere at non-LTE conditions [17].

Martian atmosphere entry

Rivière et al. [28] have modeled, with an SNB approach, the infrared radiative properties of CO/CO_2 mixtures between 500 and 5000 cm^{-1} for temperature and pressure ranges limited to 4000 K and 100 Pa respectively. For these thermophysical conditions, line broadening is mainly due to the Doppler effect. Consequently the model parameters are \bar{k} and β_D . Of the different line intensity distributions which have been tested, the exponential distribution was used, giving:

$$\frac{\overline{W_D}}{\delta} = \overline{\beta_D} E \left(\frac{\overline{k u}}{\overline{\beta_D}} \right) \quad (81)$$

where $E(y)$ is defined as:

$$E(y) = \frac{1}{\sqrt{\pi}} \int_{-\infty}^{+\infty} \frac{y \exp(-x^2)}{1 + y \exp(-x^2)} dx \quad (82)$$

Parameters have been generated from LBL calculations using a Voigt profile: the \bar{k} parameters have been obtained from spectra averaged over spectral bands and the $\overline{\beta_D}$ parameters have been adjusted on the theoretical curve of growth with a least-squares fit. CO and CO_2 parameters have been generated for a temperature grid between 1000 and 4000 K with a 200 K step. For the spectral grid, spectral bands of 25 cm^{-1} were considered.

Figure 9 shows an example of the application of the SNB model for a CO_2/CO mixture. Radiative flux has been calculated on the surface of a Martian entry vehicle (AEROFast demonstrator [19]) for a trajectory point.

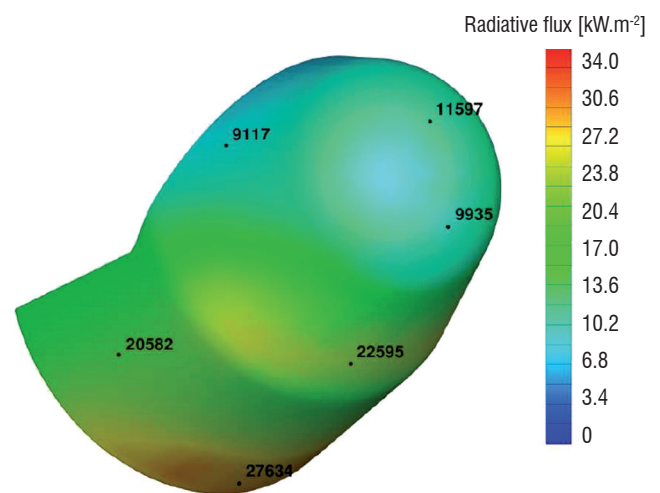


Figure 9 - Radiative flux on the surface of a Martian entry vehicle with a biconic shape.

Earth's atmosphere re-entry

Lamet et al. [18] have developed a hybrid model (SNB-box-LBL) of the radiative properties in non-LTE $N_2 - O_2$ plasmas such as those encountered on Earth re-entry. For this kind of non-LTE application, a multi-temperature approach is generally used. Transrotational (T) and electrovibrational/free electron (T_{ve}/T_e) temperatures can reach 50000 K and 25000 K respectively, and pressure conditions are about a few bar in the shock layer. Given these temperatures, the spectral interval considered is 1000 cm^{-1} to 200000 cm^{-1} .

An SNB model was formulated for optically thick (in re-entry applications) electronic systems of diatomic molecules involved in air plasmas (N_2 VUV systems, NO UV systems, and O_2 Schumann-Runge system). Considering the thermophysical conditions, the lines have a Voigt profile. The model parameters are \bar{k} , $\overline{\beta_D}$ and $\overline{\beta_L}$. Of the different line intensity distributions which have been tested, the exponential distribution and the tailed-inverse exponential distribution have been selected for the Doppler and Lorentz contributions respectively, giving:

$$\frac{\overline{W_D}}{\delta} = \overline{\beta_D} E\left(\frac{\overline{ku}}{\overline{\beta_D}}\right) \quad (83)$$

$$\frac{\overline{W_L}}{\delta} = 2\overline{\beta_L} \left(\sqrt{1 + \frac{\overline{ku}}{\overline{\beta_L}}} - 1 \right) \quad (84)$$

where $E(y)$ is given by relation (82).

The parameters have been generated from line by line calculations in the Voigt regime: the parameters \overline{k} have been obtained by averaging absorption spectra over each spectral band and the parameters $\overline{\beta_D}$ and $\overline{\beta_L}$ have been adjusted to fit expression (63) to the theoretical curves of growth. Moreover, the parameters $\overline{\eta} / \overline{\kappa}$, present in relation (20), have been calculated to take into account non-equilibrium conditions. In fact, in non-LTE conditions, this ratio, which can have significant spectral dynamics, is not equal to the Planck function. Moreover, it has been checked that there is no spectral correlation

problem between $\overline{\eta} / \overline{\kappa}$ and $\overline{\tau}$. Parameters have been tabulated for a band width equal to 1000 cm^{-1} and a two temperature grid (T, T_{ve}) .

For continua and optically thin molecular systems, a box model has been used. For the latter's contribution, mean emission and absorption coefficients have been tabulated on the same two-temperature grid. For continua, mean emission and absorption coefficients have been tabulated as functions of T_e in the range 500-25000 K [16]. Finally, for atomic lines, the line by line approach has been retained due to the unsatisfactory results obtained with an SNB model. For this contribution, Stark broadening is also taken into account since this kind of broadening is generally significant in Earth re-entry conditions (ionized plasma above 10000 K). Half-widths at half-maximum are calculated as explained in Ref. [27].

This hybrid modeling has been used to calculate, for a trajectory point, the radiative flux at the surface of an Earth re-entry probe (FIRE II [2], see Figure 10) due to radiative transfer in the shock layer. The Monte Carlo methodology has been used with 20 and 200 millions rays [17] ■

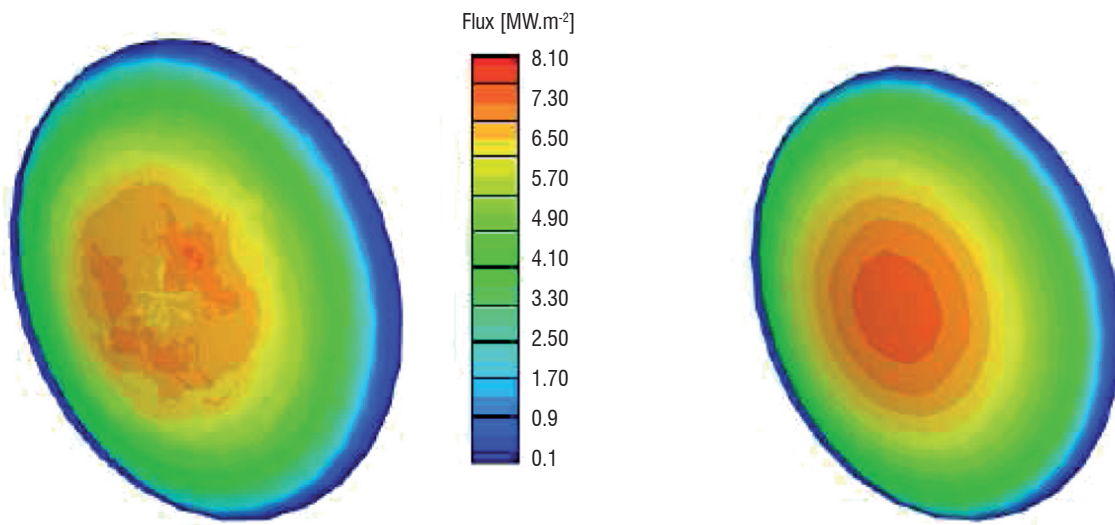


Figure 10 - Radiative flux on the front shield of an Apollo type vehicle (FIRE II [2]). Results obtained for a trajectory point with a Monte Carlo method with 20 millions rays (on the left) and 200 millions rays (on the right) [17].

Acknowledgements

The authors would like to thank Francis Dupoirieux and Luc-Henry Dorey for their contributions to the development of the radiative transfer solvers. The authors also thank the EM2C laboratory of Ecole Centrale Paris for providing gas radiative property models.

References

- [1] C. F. BOHREN and D. R. HUFFMAN - *Absorption and Scattering of Light by Small Particles*. John Wiley, New York, 1983.
- [2] D. L. CAUCHON - *Radiative Heating Results from the Fire II Flight Experiment at a Reentry Velocity of 11.4 Kilometers per Second*. Technical Report NASA TM X-1402, 1972.
- [3] S. CHAUVEAU - *Constitution de bases de données spectroscopiques relatives à un plasma d'air. Application au calcul de transfert radiatif*. Thèse de doctorat, École Centrale Paris, 2001.
- [4] P. J. COELHO - *Numerical Simulation of the Interaction Between Turbulence and Radiation in Reactive Flows*. Progress in Energy and Combustion Science, Vol. 33, pp. 311-383, 2007.
- [5] A. COPPALLE and D. JOYEUX - *Temperature and Soot Volume Fraction in Turbulent Diffusion Flames: Measurements of Mean and Fluctuating Values*. Combustion and Flame, Vol. 96, pp. 275-285, 1994.
- [6] A. REFLOCH, B. COURBET, A. MURRONE, P. VILLEDIEU, C. LAURENT, P. GILBANK, J. TROYES, L. TESSÉ, G. CHAINERAY, J.B. DARGAUD, E. QUÉMERAIS and F. VUILLOT, - CEDRE Software. Aerospace Lab Issue 2 March 2011.
- [7] M.K. DENISON and B.W. WEBB - *The Spectral Line-Based Weighted-Sum-of-Gray-Gases Model in Nonisothermal Nonhomogeneous Media*. Journal of Heat Transfer, Vol. 117, pp. 359-365, 1995.

- [8] K. V. DESHMUKH, M. F. MODEST and D. C. HAWORTH – *Direct Numerical Simulation of Turbulence-Radiation Interactions in a Statistically One-Dimensional Nonpremixed System*. Journal of Quantitative Spectroscopy and Radiative Transfer, Vol. 109, pp. 2391-2400, 2008.
- [9] L. A. DOMBROVSKY - *On Possibility of Determination of Disperse Composition of Two-Phase Flow Using Light Scattering under Small Angles*. Teplof. Vys. Temp, 1982.
- [10] F. DUPOIRIEUX, L. TESSÉ, A. AVILA and J. TAINE - *An Optimized Reciprocity Monte Carlo Method for the Calculation of Radiative Transfer in Media of Various Optical Thicknesses*. International Journal of Heat and Mass Transfer, Vol. 49, pp. 1310-1319, 2006.
- [11] R. DUVAL - *Transferts radiatifs dans les moteurs à propergol solide*. Thèse de doctorat, École Centrale Paris, 2002.
- [12] J. T. FARMER, J. R. HOWELL - *Monte Carlo Strategies for Radiative Transfer in Participating Media*. Advances in Heat Transfer, Vol. 31, pp. 1-97, 1998.
- [13] R.M. GOODY and Y.L. YUNG - *Atmospheric Radiation*. Oxford Univ. Press, New York, 1989.
- [14] H.C. HOTTEL and A.F. SAROFIM - *Radiative Transfer*. McGraw-Hill, New York, 1967.
- [15] Y. JOUMANI - *Transferts radiatifs dans les moteurs à propergol solide*. Thèse de doctorat, Université de Valenciennes et du Hainaut Cambresis, 2001.
- [16] J.-M. LAMET, Y. BABOU, PH. RIVIÈRE, M.-Y. PERRIN and A. SOUFIANI - *Radiative Transfer in Gases Under Thermal and Chemical Nonequilibrium Conditions: Application to Earth Atmospheric Re-entry*. Journal of Quantitative Spectroscopy and Radiative Transfer, Vol. 109, Issue 2, pp. 235-244, January 2008.
- [17] J.-M. LAMET - *Transferts radiatifs dans les écoulements hypersoniques de rentrée atmosphérique terrestre*. Thèse de doctorat, École Centrale Paris, 2009.
- [18] J.-M. LAMET, PH. RIVIÈRE, M.-Y. PERRIN and A. SOUFIANI - *Narrow-Band Model for Nonequilibrium Air Plasma Radiation*. Journal of Quantitative Spectroscopy and Radiative Transfer, Vol. 111, Issue 1, pp. 87-104, January 2010.
- [19] G. LEPLAT, J.-L. VÉRANT and J.-M. LAMET - *AEROFAST European Collaborative Project: Computational Aerothermodynamic Analysis of a Biconic Vehicle Design for Mars Aerocapture*. Technical Report Onera n° RT 3/14925, 2010
- [20] C.B. LUDWIG, W. MALKMUS, J.E. REARDON and J.A.L. THOMSON - *Handbook of Infrared Radiation from Combustion Gases*. Technical Report NASA SP-3080, Washington DC, 1973.
- [21] R. S. MEHTA, D. C. HAWORTH and M. F. MODEST - *Composition PDF/Photon Monte Carlo Modeling of Moderately Sooting Turbulent Jet Flames*. Combustion and Flame, Vol. 157, pp. 982-994, 2010.
- [22] R. S. MEHTA, M. F. MODEST and D. C. HAWORTH - *Radiation Characteristics and Turbulence-Radiation Interactions in Sooting Turbulent Jet Flames*. Combustion Theory and Modelling, Vol. 14, N° 1, pp. 105-124, 2010.
- [23] M. F. MODEST - *Radiative Heat Transfer*. Academic Press, 2nd edition, 2003.
- [24] M.-Y. PERRIN, PH. RIVIÈRE and A. SOUFIANI - *Radiation Database for Earth and Mars Entries*. Lecture Series on Non-equilibrium Gas Dynamics, from Physical Models to Hypersonic Flights. (RTO-AVT-VKI), 2008.
- [25] L. PIERROT - *Développement, étude critique et validation de modèles de propriétés radiatives infrarouges de CO₂ et H₂O à haute température. Application au calcul des transferts dans des chambres aéronautiques et à la télédétection*. Thèse de doctorat, École Centrale Paris, 1997.
- [26] PH. RIVIÈRE, A. SOUFIANI, M. Y. PERRIN, H. RIAD and A. GLEIZES - *Air Mixture Radiative Property Modeling in the Temperature Range 10,000-40,000 K*. Journal of Quantitative Spectroscopy and Radiative Transfer, Vol. 56, pp. 29-45, 1996.
- [27] PH. RIVIÈRE - *Systematic Semi-Classical Calculations of Stark Broadening Parameters of NI, OI, NII, OII Multiplets for Modelling the Radiative Transfer in Atmospheric Air Mixture Plasmas*. Journal of Quantitative Spectroscopy and Radiative Transfer, Vol. 73, pp. 91-110, 2002.
- [28] PH. RIVIÈRE, M.-Y. PERRIN and A. SOUFIANI - *Line-by-Line and Statistical Narrow-Band Calculations of Radiative Transfer in Some Atmospheric Entry Problems*. In Proceedings of the First International Workshop on Radiation of High Temperature Gases in Atmospheric Entry, Lisbon, pp. 189-196. ESA SP-533, 2003.
- [29] PH. RIVIÈRE. Private Communication, 2010.
- [30] M. ROGER, P. J. COELHO and C. B. DA SILVA – *The Influence of the non-Resolved Scales of Thermal Radiation in Large Eddy Simulation of Turbulent Flows: a Fundamental Study*. International Journal of Heat and Mass Transfer, Vol. 53, pp. 2897-2907, 2010.
- [31] O. ROUZAUD, L. TESSÉ, T. SOUBRIÉ, A. SOUFIANI, PH. RIVIÈRE and D. ZEITOUN - *Influence of Radiative Heating on a Martian Orbiter*. Journal of Thermophysics and Heat Transfer, Vol. 22, N° 1, pp. 10-19, January-March 2008.
- [32] R. SIEGEL and J. R. HOWELL – *Thermal Radiation Heat Transfer*. 4th edition, Taylor and Francis, New York, 2002.
- [33] A. SOUFIANI and J. TAINE - *High Temperature Gas Radiative Property Parameters of Statistical Narrow-Band Model for H₂O, CO₂ and CO, and Correlated-K Model for H₂O and CO₂*. International Journal of Heat and Mass Transfer, Vol. 40, pp. 987-991, 1997.
- [34] J. TAINE and A. SOUFIANI - *Gas IR Radiative Properties: From Spectroscopic Data to Approximate Models*. Advances in Heat Transfer, Vol. 33, pp.295-414, 1999.
- [35] L. TESSÉ - *Modélisation des transferts radiatifs dans les flammes turbulentes par une méthode de Monte Carlo*. Thèse de doctorat n°2001-34, École Centrale de Paris, 2001.
- [36] L. TESSÉ, F. DUPOIRIEUX, B. ZAMUNER and J. TAINE - *Radiative Transfer in Real Gases Using Reciprocal and Forward Monte Carlo Methods and a Correlated-k Approach*. International Journal of Heat and Mass Transfer, Vol. 45, pp. 2797-2814, 2002.
- [37] L. TESSÉ, F. DUPOIRIEUX and J. TAINE - *Monte Carlo Modeling of Radiative Transfer in a Turbulent Sooty Flame*. International Journal of Heat and Mass Transfer, Vol. 47, pp. 555-572, 2004.
- [38] L. TESSÉ, S. AVILA, F. DUPOIRIEUX and J. TAINE - *Coupled Modeling of Aerothermochemistry, Soot Formation and Radiation in a Turbulent Diffusion Flame*. In Proceedings of the 13th International Heat Transfer Conference (IHTC-13), Sydney, Australia, August 13-18, 2006.
- [39] S. J. YOUNG - *Nonisothermal Band Model Theory*. Journal of Quantitative Spectroscopy and Radiative Transfer, Vol. 18, pp.1-28, 1977.

Acronyms

CFD (Computational Fluid Dynamics)
 CG (Curtis-Godson)
 CK (Correlated-K)
 CPU (Central Processing Unit)

DNS (Direct Numerical Simulation)
 DOM (Discrete Ordinates Method)
 HWHM (Half-Width at Half-Maximum)
 HPBM (High Pressure Box Model)

LBL (Line-By-Line)
LES (Large Eddy Simulation)
LTE (Local Thermodynamic Equilibrium)
OTFA (Optically Thin Fluctuation Approximation)
PDF (Probability Density Function)

RANS (Reynolds-Averaged Navier-Stokes)
RTE (Radiative Transfer Equation)
SNB (Statistical Narrow-Band)
TRI (Turbulence-Radiation Interaction)

AUTHORS



Lionel Tessé received his Ph.D. degree, in energetics and the physics of transfer, from the École Centrale Paris in 2001. For his Ph.D. he worked on the modeling, using the Monte Carlo method, of radiative transfer in a turbulent sooty flame, focusing on the interaction between turbulence and radiation. He has been a research scientist at Onera, in the Applied and Fundamental Energetics Department, since 2001. His research topics include the modeling and simulation of radiative transfer in aeroengine combustors, solid propellant rocket motors and hypersonic flows occurring during atmospheric (re-)entries. He is in charge of the development of the ASTRE code (Monte Carlo) and is involved in the development of the REA code (DOM), both codes dedicated to radiative transfer computations.



Jean-Michel Lamet graduated from the École Supérieure d'Ingénieurs de Poitiers in 2005 and received his Ph.D. degree from École Centrale Paris in 2009. For his Ph.D. he worked on the radiative transfer in atmospheric re-entry hypersonic flows. He now holds a position of research scientist in the Onera Applied and Fundamental Energetics Department. His activity includes the modeling and simulation of radiative transfer in combustion chambers and hypersonic flows. He is involved in the development of the ASTRE and REA codes dedicated to radiative transfer.